



Calhoun: The NPS Institutional Archive
DSpace Repository

Reports and Technical Reports

All Technical Reports Collection

1978-06

A Validation of Mathematical Models for Turbojet Test Cells

Walters, John J.; Netzer, David W.

Monterey, California. Naval Postgraduate School

<http://hdl.handle.net/10945/69410>

This publication is a work of the U.S. Government as defined in Title 17, United States Code, Section 101. Copyright protection is not available for this work in the United States.

Downloaded from NPS Archive: Calhoun



Calhoun is the Naval Postgraduate School's public access digital repository for research materials and institutional publications created by the NPS community. Calhoun is named for Professor of Mathematics Guy K. Calhoun, NPS's first appointed -- and published -- scholarly author.

Dudley Knox Library / Naval Postgraduate School
411 Dyer Road / 1 University Circle
Monterey, California USA 93943

<http://www.nps.edu/library>

LEVEL

NPS67-78-002

NAVAL POSTGRADUATE SCHOOL

Monterey, California

AD A 055991

AD No. _____
DDC FILE COPY



DDC
JUL 5 1978
OFFICE

A VALIDATION OF MATHEMATICAL MODELS

FOR TURBOJET TEST CELLS

by

John J. Walters and David W. Netzer

June 1978

Approved for public release; distribution unlimited

Prepared for:
Naval Air Propulsion Center
Trenton, NJ 09628

78 07 03 004

NAVAL POSTGRADUATE SCHOOL

Monterey, California

Rear Admiral T. F. Dedman
Superintendent

Jack R. Borsting
Provost


The work reported herein was supported by the Naval Air Propulsion Center, Trenton, NJ, as part of the Naval Environmental Protection Technology Program.

Reproduction of all or part of this report is authorized.

This report was prepared by:



JOHN J. WALTERS, LT, USN

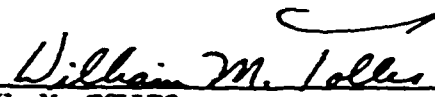


DAVID W. NETZER
Associate Professor of Aeronautics

Reviewed by:



R. W. SELL, Chairman
Department of Aeronautics



W. M. TOLLES
Acting Dean of Research

UNCLASSIFIED

SECURITY CLASSIFICATION OF THIS PAGE (When Data Entered)

REPORT DOCUMENTATION PAGE		READ INSTRUCTIONS BEFORE COMPLETING FORM
1. REPORT NUMBER NPS-67Nt78061	2. GOVT ACCESSION NO.	3. RECIPIENT'S CATALOG NUMBER
4. TITLE (and Subtitle) A VALIDATION OF MATHEMATICAL MODELS FOR TURBOJET TEST CELLS		5. TYPE OF REPORT & PERIOD COVERED Final, 1978
7. AUTHOR(s) John Justin Walters Davis N. Netzer D. W. Netzer		6. PERFORMING ORG. REPORT NUMBER
8. PERFORMING ORGANIZATION NAME AND ADDRESS Naval Postgraduate School Monterey, CA 93940		9. CONTRACT OR GRANT NUMBER(s)
10. CONTROLLING OFFICE NAME AND ADDRESS Naval Air Propulsion Center Trenton, NJ		13. PROGRAM ELEMENT, PROJECT, TASK AREA & WORK UNIT NUMBERS N62378WR00013
14. MONITORING AGENCY NAME & ADDRESS (if different from Controlling Office)		12. REPORT DATE June 1978
		13. NUMBER OF PAGES 61 (12) 5901
		15. SECURITY CLASS. (of this report) UNCLASSIFIED 15a. DECLASSIFICATION/DOWNGRADING SCHEDULE
16. DISTRIBUTION STATEMENT (of this Report) Approved for public release; distribution unlimited		
17. DISTRIBUTION STATEMENT (of the abstract entered in Block 20, if different from Report)		
18. SUPPLEMENTARY NOTES		
19. KEY WORDS (Continue on reverse side if necessary and identify by block number) Turbojet Test Cell Mathematical Model Validation		
20. ABSTRACT (Continue on reverse side if necessary and identify by block number) Previously developed one-dimensional and two-dimensional computer models for predicting turbojet test cell performance were compared with data obtained from a subscale test cell for the purpose of model validation. Comparisons were made for a variety of configurations and flow rates. A modified one-dimensional model was found to reasonably predict the variation of augmentation ratio with engine flow rate, although predicted magnitudes were consistently too small. The model incorporated excess ve drag losses and an inaccurate jet spreading parameter for large engine-augmentor spacings. The two-dimensional model accurately predicted		

UNCLASSIFIED

SECURITY CLASSIFICATION OF THIS PAGE (When Data Entered)

experimental velocity profiles, but over-predicted pressure variations, except for low engine exit Mach numbers.

NO	DATE	BY
100	10/15/73	W. J. ...
EXTENSION ...		
BY		
EXTENSION ...		
DATE		
A		

DD Form 1473
1 Jan 73
S/N 0102-014-6601

UNCLASSIFIED

SECURITY CLASSIFICATION OF THIS PAGE (When Data Entered)

TABLE OF CONTENTS

<u>Section</u>	<u>Page</u>
I. INTRODUCTION	1
II. METHOD OF INVESTIGATION	6
III. EXPERIMENTAL APPARATUS	7
A. TEST CELL.	7
B. ENGINE AND AUGMENTOR	8
C. INSTRUMENTATION	8
D. DATA ACQUISITION	9
IV. EXPERIMENTAL PROCEDURES	10
A. TEST PROCEDURES	10
B. DATA REDUCTION	10
C. TEST CONDITIONS	12
V. MODELS TESTED	13
A. ONE-DIMENSIONAL MODEL	13
B. TWO-DIMENSIONAL MODEL	15
VI. RESULTS AND DISCUSSION	17
A. ONE-DIMENSIONAL MODEL	17
B. TWO-DIMENSIONAL MODEL	19
VII. CONCLUSIONS AND RECOMMENDATIONS	22
A. ONE-DIMENSIONAL MODEL	22
B. TWO-DIMENSIONAL MODEL	23
LIST OF REFERENCES	51
INITIAL DISTRIBUTION LIST	52

LIST OF TABLES

I. TEST CONDITIONS 12

LIST OF FIGURES

1. CELL TEST SECTION	24
2. AUGMENTOR TUBE AND STACK TRANSLATION APPARATUS	25
3. END VIEW OF TEST SECTION (FACING UPSTREAM)	26
4. ENGINE-AUGMENTOR INTERFACE GEOMETRY	26
5. AUGMENTOR INLET VARIATIONS	27
6. ONE-DIMENSIONAL MODEL GEOMETRY	27
7. AUGMENTATION RATIO VS. SPACING (TEST CELL)	28
8. AUGMENTATION RATIO VS. SPACING (MODEL)	29
9. AUGMENTATION RATIO VS. FLOW RATE (TEST CELL)	30
10. AUGMENTATION RATIO VS. FLOW RATE (MODEL)	31
11. AUGMENTATION RATIO VS. FLOW RATE, ZERO SPACING	32
12. AUGMENTATION RATIO VS. FLOW RATE, 1.12D SPACING	32
13. AUGMENTATION RATIO VS. FLOW RATE, 2.12D SPACING	34
14. AUGMENTATION RATIO VS. FLOW RATE, 3.12D SPACING	35
15. AUGMENTOR VELOCITY PROFILES: FLOW RATE = 1.0; SPACING = 0; AUGMENTATION RATIO = 1.26; COLD FLOW	36
16. AUGMENTOR VELOCITY PROFILES: FLOW RATE = 1.0; SPACING = 1 NOZZLE DIAMETER; AUGMENTATION RATIO = 1.52; COLD FLOW	37
17. AUGMENTOR VELOCITY PROFILES: FLOW RATE = .99; SPACING = 2 NOZZLE DIAMETERS; AUGMENTATION RATIO = 1.55; COLD FLOW	38
18. AUGMENTOR VELOCITY PROFILES: FLOW RATE = 1.52; SPACING = 1 NOZZLE DIAMETER; AUGMENTATION RATIO = 1.29; COLD FLOW	39
19. AUGMENTOR PRESSURE PROFILE, FLAT INLET, ZERO SPACING	40
20. AUGMENTOR PRESSURE PROFILE, FLAT INLET, ZERO SPACING	41
21. AUGMENTOR PRESSURE PROFILE, FLAT INLET, 1-D SPACING	42
22. AUGMENTOR PRESSURE PROFILE, FLAT INLET, 1-D SPACING	43
23. AUGMENTOR PRESSURE PROFILE, FLAT INLET, 2-D SPACING	44
24. AUGMENTOR PRESSURE PROFILE, FLAT INLET, 2-D SPACING	45

25. AUGMENTOR PRESSURE PROFILE, FLAT INLET, 1-D SPACING, HOT FLOW	46
26. AUGMENTOR PRESSURE PROFILE, STRAIGHT INLET, ZERO SPACING . . .	47
27. AUGMENTOR PRESSURE PROFILE, STRAIGHT INLET, ZERO SPACING . . .	43
28. AUGMENTOR TEMPERATURE PROFILE, FLAT INLET, 1-D SPACING	49
29. AUGMENTOR TEMPERATURE PROFILE, FLAT INLET, 2-D SPACING	50

PRECEDING PAGE BLANK-NOT FILMED

I. INTRODUCTION

Accurate, controlled testing of high technology jet engines requires a fixed installation where such engines may be operated throughout their full thrust envelope under conditions approximating the installed situation, and with sufficient instrumentation to assess performance parameters. These installations, jet engine test cells, have taken many forms, among them the "Hush-House" installed at NAS Miramar, CA [Ref. 1] for installed engine testing, and a Coanda design [Ref. 2] for noise suppression. The most common cell design is typically a block house type installation with vertical inlet and exhaust stacks configured for velocity profile and noise control. Arrangements with horizontal inlet and exhaust stacks exist and provide more uniform flow profiles to the engine inlet, but the large clear areas needed adjacent to this type cell precludes its frequent use. Mounting hardware and monitoring equipment are provided as appropriate to the engine under test.

Pollution control is a major problem in the operation of cells with today's high power, high mass flow engines. Noise and visible and invisible pollutants are emitted in quantity. Judicial action initiated by the State of California against Naval Air Station facilities in California has brought these problems into prominence. Atmospheric pollution has been attacked using various forms of water droplet adhesion, mechanical grid entrapment, or electronic ionization, with baffle combinations for acoustic treatment [Ref. 3]. Good results have been obtained at NAS Jacksonville, FL, with a water scrubbing technique to remove pollutant particles. All these methods are expensive and complicated, however, and simpler ones are desired. To find them will require a detailed understanding of test cell aerodynamics.

In a basic arrangement the engine is situated somewhere near the center of the cell to allow a near uniform flow profile to develop. It exhausts into an augmentor tube where more air is entrained from within the cell, causing air to flow around the engine into the augmentor tube. The ratio of entrained air mass flow rate to engine mass flow rate is known as "augmentation ratio." The entrained "secondary air" acts as a coolant for the hot engine gases, extending exhaust stack life, and as a diluent for the exhaust products. Augmentor parameters such as engine-augmentor spacing and augmentor diameter are important to proper cell/engine operation due to their effect on augmentation ratio. An excessively high augmentation ratio (high secondary air flow) may cause large pressure gradients between engine inlet and exhaust planes with resulting inaccurate performance measurements. In addition, test cell structural limits might be exceeded due to excessive cell pressure reduction. Insufficient secondary air could allow hot exhaust gas recirculation to the engine inlet with performance degradation as well as hot spots in the augmentor tube and exhaust stacks. Insufficient secondary air flow also causes excessive density of visible emittants. This may violate Ringleman Number limitations of local pollution ordinances even when the pollutant output quantities are within specified limitations.

Testing for optimization of engine-augmentor relationships cannot easily be accomplished in existing, operational test cells. Cells are scheduled to maximum capacity for economy reasons, making test runs inconvenient. Also, today's large engines and soaring fuel costs make full scale testing prohibitively expensive. Clearly, computer modeling of flows provides a possible alternative.

A working, proven model would be able to predict augmentation ratios and recirculation of hot engine exhaust gases as a function of augmentor design.

It could provide information on the optimal locations for water quenching devices needed to cool hot afterburner exhaust flows and jet break-up devices used for noise suppression purposes. These capabilities would reduce the requirement for expensive, time consuming, trial and error procedures now used.

A number of models with some or all of these capabilities are in existence. One by United Research Laboratories [Ref. 4] uses a one-dimensional idealization combined with empirical correlation factors to adjust output values of exit static and total pressure (to agree with experimental results), then generates performance data for various augmentor combination. Eliin and Pucci [Ref. 5] attacked a similar problem in modeling a gas eductor system for gas turbine powered ships. Due to differences in application, however, this model made no allowances for spacing between nozzle exhaust and tube inlet, a commonly found configuration in test cells. Bailey [Ref. 6] also used the one-dimensional idealization and accounted for friction and inlet losses through empirical data and engine-augmentor spacing by means of theoretical spreading equations [Ref. 7] for the engine exhaust stream. Hasinger [Ref. 8] also utilized a one-dimensional model to perform a study of aircraft ejector optimization. The problem was also approached using two-dimensional theory by Hayes and Netzer [Ref. 9] and by Croft and Lilley [Ref. 10].

Experimental validation of the 1-D model of Bailey [Ref. 6] and the 2-D model of Hayes and Netzer [Ref. 9] was the subject of this study. The one-dimensional Bailey model is simple and uses little computer time. It relies heavily on empirical loss factors which are applied to flow conditions different from the original experiments. It is fundamentally restricted to calculation of trends of augmentation ratio with variations in engine flow rate, engine augmentor spacing, engine diameter, and augmentor diameter. It has, on the other hand, no restrictions to conditions of application. It

incorporates corrections for choked flow at the engine nozzle and the basic one-dimensional equations for mass, energy, and momentum conservation are not limited by Mach number. It does not, however, incorporate provisions for handling exhaust shocks, or jet spreading for choked flow conditions.

The two-dimensional model supplies a far more complete data set. It predicts temperatures, velocities, pressures, and turbulence levels throughout the flow field within the augmentor tube and parts of the test cell. It is a more rigorous solution of the basic conservation equations and relies on empirical constants only for the turbulence modeling and boundary conditions on vorticity. It is limited by an assumption of incompressible flow (more accurately, density is assumed to vary with temperature and composition but not with pressure) which prevents accurate results above flow Mach numbers of about 0.6. It is additionally weakened by the use of stream function and vorticity as primary variables. These variables make the solution simpler by eliminating pressure from the equations and by reducing the dependence on velocities. However, the recovery of pressure from the solution is extremely sensitive to calculations for the stream functions. Both these areas can be strengthened by new computation techniques. These include elliptic equations which reduce to parabolic in appropriate conditions and the use of pressure and temperature as primary variables. These techniques are currently being investigated at the Naval Postgraduate School.

All test cell models in existence which are available in the open literature have the same basic drawback — none have been experimentally validated over the normal range of test conditions found in actual test cells. Due to the wide range of assumptions incorporated in the models, and the unusual flow conditions found in jet engine exhausts (hot, high velocity core entraining cold, stationary air), models must be tested against experimental data before

they can be used with any confidence. Testing should include measurement of velocity profiles in the test cell and augmentor tube to test the validity of inlet and exit profile assumptions made in all models and the accuracy of flow field velocity computations in the two-dimensional models. Accurate measurements of flowrates and augmentation ratio are necessary to provide inputs to the 2-D model and to check predicted results in the 1-D model. Pressures and temperatures along the augmentor tube and in the test cell must be measured to provide data for comparison to 2-D predictions.

To make all these measurements in a full scale operational cell would be time consuming and costly for the same reasons mentioned earlier. For these reasons, the subscale test cell designed and built at the Naval Postgraduate School [Ref. 11] was chosen for validation efforts. It is substantially less expensive and more convenient to operate and can easily and inexpensively be completely instrumented. Configurations can be quickly varied and data easily and rapidly collected and reduced.

II. METHOD OF INVESTIGATION

A previously constructed one-eighth scale turbojet test cell [Ref. 11] was modified to increase the quantity of obtainable data, and used in a validation study of two test cell flow models. A one-dimensional and a two-dimensional model were evaluated. The cell was used to determine the effects of engine-augmentor spacing, engine mass flow rate, engine nozzle total temperature and augmentor inlet geometry on augmentation ratio and augmentor pressure, velocity, and temperature distributions. Experimentally measured pressure, temperature, and velocity profiles were compared with theoretical predictions.

III. EXPERIMENTAL APPARATUS

A. TEST CELL

Design and construction of the subscale turbojet test cell are detailed in Ref. 11 and shown in Figs. 1 and 2. The cell is a one-eighth scale model of a NAS Alameda test cell. A TF41 engine was scaled to one-eighth in diameter resulting in mass flow being scaled by $1/64$ to maintain flow velocities equal to those in the full scale cell. Air was drawn into the test section through a horizontal inlet with square bellmouth and a flow straightening section. The test section was enclosed by hinged plexiglass sides to allow easy access and visual monitoring of the section during operation. The augmentor tube, equipped for interchangeable inlets, exited the cell through a removable wall. Its downstream end was attached to a deflector-plate-equipped vertical exhaust stack. The stack was mounted on a wheel/rail arrangement which allowed translation of the stack/augmentor assembly and resulted in changes in spacing between the engine and augmentor tube. Removable metal grates were installed in the stack to permit variation in back pressure.

The engine used to simulate turbojet/turbofan tailpipe and nozzle conditions was a forced air ramjet supplied with compressed air from an Allis-Chalmers, twelve-stage axial compressor. Separate three-inch pressure lines supplied variable combustor (primary) and bypass (secondary) air. The engine intake was simulated by a variable suction six-inch line drawing through a six-inch bellmouth. The combustor was a sudden expansion (or dump) type fed by nitrogen-pressurized JP4 and ignited by a methane-oxygen torch in the combustor wall. The arrangement allowed control of tailpipe flow rate, nozzle total temperature and pressure, and nozzle geometry.

B. ENGINE AND AUGMENTOR

Figure 3 shows the basic placement of the ramjet in the test section when viewed from downstream. Figure 4 shows the geometry of the engine-augmentor interface. Mass flow rate could be controlled independently in the primary and secondary lines, providing a simulation of a variable bypass turbofan, if desired. Mixing of the primary and secondary streams was, unfortunately, not as complete as in an actual turbofan and in hot runs the arrangement resulted in a hot inner core of primary air surrounded and pinched by cold secondary air. Lengthening of the mixing section will eliminate this problem in the future. Engine-augmentor spacing was varied by rolling the exhaust stack along its rails. The three augmentor tube inlets primarily tested (Fig. 5) were separate pieces, easily changed by the removal of two screws.

C. INSTRUMENTATION

Flow rates in the three-inch primary and secondary and six-inch suction lines were measured using ASME type flow orifices and controlled by hand valves. Pressure taps and thermocouples in the test cell allowed monitoring of pressures at the engine inlet and exhaust planes and ambient air temperatures. A pressure tap and iron-constantan thermocouple in the combustor outer wall allowed calculation of nozzle total temperature and pressure. Augmentor flow conditions were monitored by 27 pressure taps along the top of the tube, spaced at one-inch intervals near the upstream and downstream ends, spreading to four inches near the center. Twelve copper-constantan thermocouples were also placed along the tube at four-inch intervals. All thermocouples were referenced against an ice water bath. Velocity profiles in the augmentor were measured with a pitot rake consisting of seven equally spaced small diameter total pressure tubes. The rake could be rotated and translated to obtain vertical and

horizontal profiles over the full length of the tube. A thermocouple was also mounted on the center pitot tube. Velocity profiles in the cell were measured by means of a direct reading anemometer with hot wire probe. The probe had been extended sufficiently to allow measurement across the entire height and width of the cell.

D. DATA ACQUISITION

The data acquisition system consisted of a fully programmable Hewlett-Packard desk top calculator with a HP9867B Mass Memory, HP-9862A Plotter, and digital tape reader. A B. and F. Model SY133 data logger scanned 48 pressure and 20 temperature channels per run and punched raw data onto a paper tape for reading into the Hewlett-Packard system. The data reduction system produced reduced flow rates, augmentation ratio, temperatures, and pressures and automatically plotted augmentor pressure and temperature profiles.

IV. EXPERIMENTAL PROCEDURES

A. TEST PROCEDURES

Initial cell startup required about one hour for warmup of the Allis-Chalmers compressor. Once air was directed through the lines, ten to fifteen minutes were required for temperature stabilization at the flow orifices before accurate flow rates could be set. Once the desired mechanical configuration of the cell was fixed, flow rates were adjusted. Rough adjustments were made using water manometers located at the hand valves. Final adjustments were made by running flow rate data through the data reduction system and checking calculated values. When the proper values were attained, a complete set of data was processed by setting the B. & F. data logger to scan the 40 pressure and 20 temperature channels. The raw data was recorded on punched tape. The tape was then read into the data reduction system for a complete data readout. When cell velocity profiles were desired, they were obtained by manually reading and recording the probe measurements as it was inserted through the side or top of the cell. The pitot rake was also repositioned manually when velocity profiles at more than one tube position were measured.

B. DATA REDUCTION

Existing programs for the HP9830A calculator were modified to handle increased data quantity and extract more information from the raw data. Flow rates were calculated using ASME equations for D-5D orifice pressure tap configurations. Temperatures were obtained by curve-fitting published thermocouple data. Pitot rake pressures were combined with tube wall pressure and temperature measurements to calculate the velocity profile at each position of the rake. This velocity profile was then integrated by Simpson's rule to find the average flow velocity in the tube. The velocity profile at the aft end of the

augmentor tube was quite flat and varied only slightly in the tangential direction. For all tests conducted, the average velocity at this location was used to determine the flow rate through the augmentor tube. This flow rate, together with the measured engine flow rate, allowed calculation of the augmentation ratio. During the initial phase of the investigation, the augmentation ratio determined in the above manner was validated against the value determined from the test cell velocity profile. A routine was included in the program to automatically plot tube pressure and temperature profiles when desired.

C. TEST CONDITIONS

Data were taken for the set of test conditions presented in Table 1. The bellmouth data were used for 1-D model validation and the flat and straight augmentor inlet data were used for 2-D model validation.

TABLE I
TEST CONDITIONS

INLET	NOZZLE FLOW RATE (lb _m /sec)	ENG-AUG SPACING	ENG-INLET SPACING
Bellmouth	1.0	0	-1.12D
	1.5		
	2.0		
	2.3		
	1.0	1.12D	0
	1.5		
	2.0		
	2.3		
	1.0	2.12D	1D
	1.5		
	2.0		
	2.3		
1.0	3.12D	2D	
1.5			
2.0			
2.3			
Flat	1.0	0	
	1.0 (Hot)		
	1.5		
	1.0	1D	
	1.0 (Hot)		
	1.5		
Straight	1.0	2D	
	1.0 (Hot)		
	1.5		
	1.0	0	
	1.5		
	1.5		

V. MODELS TESTED

A. ONE-DIMENSIONAL MODEL

The one-dimensional model tested was described by Bailey in Ref. 6.

Geometry is shown in Figure 6.

The model assumptions were:

1. one-dimensional, steady
2. adiabatic
3. flow uniform at cross sections 1, 2, and 3
4. all gases ideal
5. mixing occurs in a constant area
6. $P_1 = P_2$
7. $A_1 + A_2 = A_3$

Values of tube and engine nozzle diameters, nozzle total temperature and pressure, and secondary air total temperature were input. A value of nozzle exit static pressure (P_1) was set, which set P_2 , and bypass air total pressure (P_{T2a}) was assumed as atmospheric. Initially, P_{T2} was set equal to P_{T2a} . From these, the model calculated the Mach numbers, and velocities at 1 and 2. The loss across the augmentor inlet was then calculated using an empirical loss constant for the particular inlet being employed. This resulted in a new value of P_{T2} and the process was repeated until successive changes in P_{T2} became small. Primary (1) and secondary (2) mass flow rates were calculated and used to solve the one-dimensional equations of momentum and energy between 1/2 and 3.

Spreading of a subsonic jet with engine augmentor spacings greater than zero was handled by use of a spreading parameter to determine the size of the mixing zone at the entrance to the augmentor tube. Velocity profiles within the mixing zone were modeled by an error function. The mixing zone was broken into a large number of small areas and then properties in each were calculated

and summed to solve the one-dimensional equations. In the case of choked flow (for 1-D isentropic conditions) in the nozzle, a correction for choking was applied to the nozzle flow rate and, for the zero spacing case, the problem was handled as before. No attempt was made in the original model to handle the choked flow case at spacings greater than zero.

Augmentor tube wall friction in the model was approximated using an equation for a flat plate drag coefficient. The drag coefficient was calculated using a Reynold's Number based on augmentor length and $\bar{V} = (V_3 + V_2)/2$ and $\bar{T} = (T_3 + T_2)/2$ (for determination of viscosity). Although not mentioned in the text of Ref. 6, an empirical coefficient was found in the equation in the program listing which arbitrarily reduced the wall friction value. The coefficient proved essential to successful operation of the model since without it, the calculated flow resistance was so high that reverse flow was predicted in the tube for all cases tested. The use of the lower value of wall friction apparently is necessary because of the considerable difference in flat plate velocity profiles from the developing coaxial flow within the augmentor tube.

To use the model as written, values of nozzle total temperature and pressure and secondary air total temperature are input with geometries and the head loss factor for the tube inlet. The published listing was modified slightly to allow entering the experimentally obtained value of back pressure (P_3). In the original model, solutions were obtained for a number of arbitrarily set values. The model then calculates primary and secondary flow rates and augmentation ratio. It is simple to use and requires minimal computing time. At the same time, it depends heavily on empirical constants for inlet losses and wall friction and the "plug flow" assumption is questionable in the case of high velocity entrance flows. It provides insight only into overall behavior, with little indication of behavior within the tube and no information on flow patterns in the test cell itself.

The model has previously been tested in a 1/24th scale plexiglass cell [Refs. 6 and 12]. Bailey found the model reasonably predicted the effects of nozzle total pressure on augmentation ratio and the variation of secondary mass flow with primary mass flow. The region of choked nozzle flow was not investigated since no provision was made to compute the spread of a supersonic exhaust stream. He discovered that published head loss factors caused excessive inlet losses and predictions were most accurate with a loss factor of essentially zero. No conclusive results were obtained for tests of engine-augmentor spacing effects on augmentation ratio due to widely scattered experimental data.

B. TWO-DIMENSIONAL MODEL

The two-dimensional model tested was described by Hayes and Netzer in Ref. 9. The model solved the basic equations of mass, momentum, and energy in two-dimensional, elliptic form. Stream function and vorticity were the primary variables for mass and momentum effects which reduced coupling problems and made equation solution easier. Temperature was the dependent variable for energy conservation. Kinetic heating was ignored and specific heat was considered constant. Turbulence effects were included in the form of a two parameter model describing the effective viscosity. The relationship used was:

$$\mu_{\text{eff}} = C_{\mu} \frac{\rho K^2}{\epsilon}$$

where:

μ_{eff} = effective viscosity

C_{μ} = empirical coefficient

ρ = local density

K = turbulence kinetic energy

ϵ = turbulence energy dissipation rate

The equations for K and ϵ were written in elliptic form and the five equations were solved with the perfect gas law to describe the flow field. Once the solution converged, axial and radial pressure distributions were obtained from the stream function distribution.

The equations were solved using point-by-point Gauss-Seidel with under-relaxation. The model was assumed axisymmetric, and described by a 43 by 40 grid in cylindrical coordinates. A flat augmentor inlet lip (Fig. 5) was included in the model as an approximation to the bevelled inlets found in some cells at NARF Alameda. The straight pipe was approximated by making this lip very small.

The model had several limitations. The elliptic equations using stream function and vorticity are inherently limited to low subsonic speeds. In addition, the use of stream function and vorticity as primary variables made calculated pressures extremely sensitive to small errors in convergence. The rectangular grid system does not allow modeling of rounded, bellmouth type inlets commonly found in operation. Solution required an average of 170 minutes CPU time on an IBM 360-67 computer. On the plus side, it is a potentially valuable tool for predicting effects of engine-augmentor spacing, augmentor diameter, and cell geometry on pressure, velocity, and temperature distributions within the test cell and augmentor at low engine flow settings. This information is needed for optimization of noise suppression and chemical pollution abatement techniques.

VI. RESULTS AND DISCUSSION

A. ONE-DIMENSIONAL MODEL

As discussed above, the model developed by Bailey was not applicable for choked nozzle flow at other than zero engine-augmentor spacing. In the model, choking was assumed to occur for the one-dimensional isentropic pressure ratio ($\gamma = 1.4$) of 1.89. The flow in converging nozzles with 25° half angles (as used in these experiments) does not actually become independent of back pressure until nozzle pressure ratios in excess of 2.5 [Ref. 13] are obtained. This results from three-dimensional effects (radial momentum, etc.) which cause the lines of constant Mach number to be convex in shape as the flow exits the nozzle. In the experiments conducted in this investigation, pressure ratios did not exceed 2.4. For these pressure ratios, the flow at the nozzle exit plane would actually be slightly subsonic. The flow would continue to accelerate to sonic or slightly supersonic flow conditions with resulting weak expansion and compression waves. Since the expansion and compression waves are quite weak for these low pressure ratios, a good approximation for the jet behavior may be to neglect them entirely and assume that the jet continues to accelerate until the jet pressure equals the local ambient pressure a short distance from the nozzle exit plane. The jet behavior could then be approximated by considering it to spread in the same manner as employed by Bailey for the subsonic jet. This modification was incorporated into the 1-D model.

The original model generally predicted trends in cell performance correctly, although with some severe limitations. Effects of engine-augmentor spacing on augmentation ratio are shown in Figs. 7 and 8 for the test cell and model, respectively. The predicted augmentation ratios were consistently lower than the experimental values. Experimentally, cell augmentation ratio was

found to decrease slightly and then level off with increased spacing (Fig. 7). The level off at increased spacing indicates that jet spreading probably became negligible at a point about two nozzle diameters downstream. The decrease found at zero spacing probably resulted from flow interference by the mounting flange of the engine nozzle which, at these separations, was very near the tube inlet. The model, which predicts continued jet spread for any distance from the nozzle, did not predict the leveling off found experimentally and could not predict the decrease caused by flange blockage. Limiting the jet spreading to that which occurs at a distance of 1.5 nozzle diameters did raise the predicted augmentation ratio for large engine-augmentor spacings (Fig. 8).

The model correctly predicted the effect of changing flow rate on augmentation ratio. Figure 9 shows that augmentation ratio decreased steadily with increasing flow rate in the test cell and Fig. 10 shows the same trend for the model.

As mentioned above, the model predictions for augmentation were consistently less than the measured values. This is more evident in Figures 11 through 14 for different engine-augmentor spacings. The prediction error was greater for the lower nozzle flow rates. Eliminating augmentor inlet losses had only small effects on the predicted augmentation ratio for zero engine-augmentor spacing (Fig. 11). Eliminating wall friction raised the predicted values to agree with experiment at low flow rates but to overpredict at high flow rates. The latter was probably due to the blockage to the secondary flow provided by the expanding jet exhaust in the experiments.

Additional comparisons are presented in Fig. 14 for a 3.12D engine-augmentor spacing. Again the basic model predicted the correct trends but

underpredicted the magnitude. The model predictions are seen to be very sensitive to the experimental input values of augmentor exhaust pressure (which depend upon exhaust stack resistance). A change of 0.1% in back pressure changes augmentation ratio by approximately 3%. Apparently this is the most important parameter in the model for obtaining the correct magnitudes of augmentation ratio. Limiting the jet spreading to that which existed at a distance of 1.5 jet diameters also increased the predicted values as did reducing wall friction.

In general, results agreed with those found by Bailey for subsonic flow and showed the same trends when the original assumptions were applied to conditions which would be choked in 1-D calculations. The model predicted trends accurately but requires improved wall friction and jet spreading calculations.

B. TWO-DIMENSIONAL MODEL

Predictions using this model were generally very accurate when it was operated within its design limitations. Elliptic type equations using the stream function-vorticity variables are generally unreliable for high subsonic velocities, since density is not considered to vary with pressure (which has been removed from the equations). Model flow rates of 1.0 lb_m/sec. resulted in a nozzle exit Mach of about 0.57 in cold flow. The higher flow conditions at 1.5 lb_m/sec. produced an exit Mach of about 0.86. Difficulty was experienced in running comparisons of the 1.0 flow rate when high nozzle total temperatures (hot flow) were employed. The model requires nozzle exit static temperature as an input parameter. An accurate value for this temperature was impossible to determine from the experiments since the exhaust jet consisted of a hot inner core at greater than 2000°R surrounded by a cool blanket of near ambient secondary air. After some unsatisfactory trial and error, an average exit

temperature of 900°R was assumed for all hot runs. This corresponded to an exit Mach of about 0.8.

Velocity profile predictions for cold flow in the augmentor with a flat plate orifice inlet were in good agreement with experiment (Figs. 15 through 18). The model does seem to consistently predict a slightly slower flattening of the profile than actually occurred since it consistently overestimated peak velocities far downstream and underpredicted close to the nozzle. The least accurate prediction was at the intake lip for the zero spacing case (Fig. 15). This is most likely due to the extreme blockage of the flow at the tube lip in the experimental setup. Since the calculated velocity must be extracted from stream function values, any error in calculation of the streamlines in this rapidly converging region would be somewhat amplified in the velocity calculation. As anticipated, prediction error was slightly greater in the high flow rate case (Fig. 18). This was not surprising since "pinching" of the nozzle flow caused a predicted centerline acceleration to a flow Mach number of 1.12, about 2.5 nozzle diameters down the augmentor. Surprisingly, in this case, the model predicted peak velocity at the tube inlet to within 3%.

Pressure predictions (Figs. 19 through 27) were in relatively good agreement with experiment, although not so impressive as the velocity results. Pressure profiles were calculated along 5 different axial grid lines of the tube, ranging in position from near centerline to about mid-radius. The outermost lines were just inside the edge of the lip of the flat intake (Ref. 9). The line J=17 (the second outermost) was found most accurate for cases with the lip installed while J=18, (slightly farther out) better fit those cases with no inlet (Figs. 26 and 27). The better accuracy is found to occur along axial lines that penetrate the upstream flow in the least disturbed (more axial flow) region. In addition,

accuracy is generally good at the low flow rates but degrades markedly at higher mass flows. These results were expected since the need to extract pressure field information from the streamline solution through two successive approximate derivative calculations renders pressures extremely sensitive to small errors in the streamlines. This sensitivity is especially evident in the figures where the pressure drop in the entrance section of the augmentor tube is consistently over predicted, the error being more significant for the high flow rates.

The model proved ineffective in predicting hot flow results. An example (Fig. 25) shows the standard result — a grossly excessive pressure drop accompanied by insufficient rise to match downstream values. Analysis of model predictions showed the nozzle flow had accelerated from a Mach of 0.8 at the nozzle exit to a value greater than Mach 1.2 along the centerline, a flow region where the model is not valid.

Results were similarly poor for hot flow temperature predictions, (Fig. 28) where data was non-dimensionalized using the maximum temperature of the run to compensate for the recognized inaccuracy of input flow temperature. While the model consistently predicted gradual mixing with maximum tube wall temperature at the downstream end, the experimental data consistently showed peak temperature at about one-third the length of the tube from the upstream end. The discrepancy in these temperature profiles is probably attributable to both the high flow Mach numbers and the poorly defined experimental nozzle exit temperature and velocity distributions as discussed above. In the cold flow case (Fig. 29), agreement was excellent.

VII. CONCLUSIONS AND RECOMMENDATIONS

A. ONE-DIMENSIONAL MGDEL

The model tested has several advantages over the more elaborate 2-D version. It used little computer time and was, therefore, very significantly less expensive to operate. It also was applicable over a wider range of conditions, not being inherently limited to low subsonic speeds. The model was not capable of accurate quantitative predictions in any flow condition, but, with an assumption of no physical choking at the nozzle exit and only weak external expansion and compression waves, it predicted trends accurately up to flow Mach numbers of about 1.2. The model can be made to closely fit experimental data by adjustments of empirical constants (wall friction, jet spreading) and then be used to consistently predict conditions for a given installation. Predictive accuracy was very sensitive to augmentor tube exhaust pressure which in turn is a function of flow rate and exhaust stack resistance.

The heavy dependence on empirical data in the model weakens its potential value as a general design tool since required constants may change from installation to installation. Loss factors for unusual configurations, such as the bevelled augmentor inlets found at NARF Alameda, could only be determined by additional experimental measurements. The subscale test cell utilized in this project can potentially be used to alleviate this shortcoming by providing an inexpensive and convenient test device to establish data for virtually any configuration. Validation of at least some selected conditions against full-scale test cell data will be required.

B. TWO-DIMENSIONAL MODEL

This model is inherently limited to low subsonic flow conditions, a situation which renders it unusable in its present form as a design tool for high thrust and afterburning conditions. Its quantitative accuracy, in its limited flow region, is very good when predicting velocities in the augmentor tube, but somewhat weaker when predicting pressures due to the need to extract them from stream function information. The model used a large amount of computing time but provided an enormous amount of detailed information on cell performance as a function of cell design and engine operating conditions.

The greatest value of the model probably lies in its function as a stepping stone to more advanced 2-D models. Current work is being directed toward a model which utilizes velocities and pressure as the primary variables. This model should improve both the accuracy and utility of the 2-D model and should provide reasonable solutions for the choked flow operating conditions.

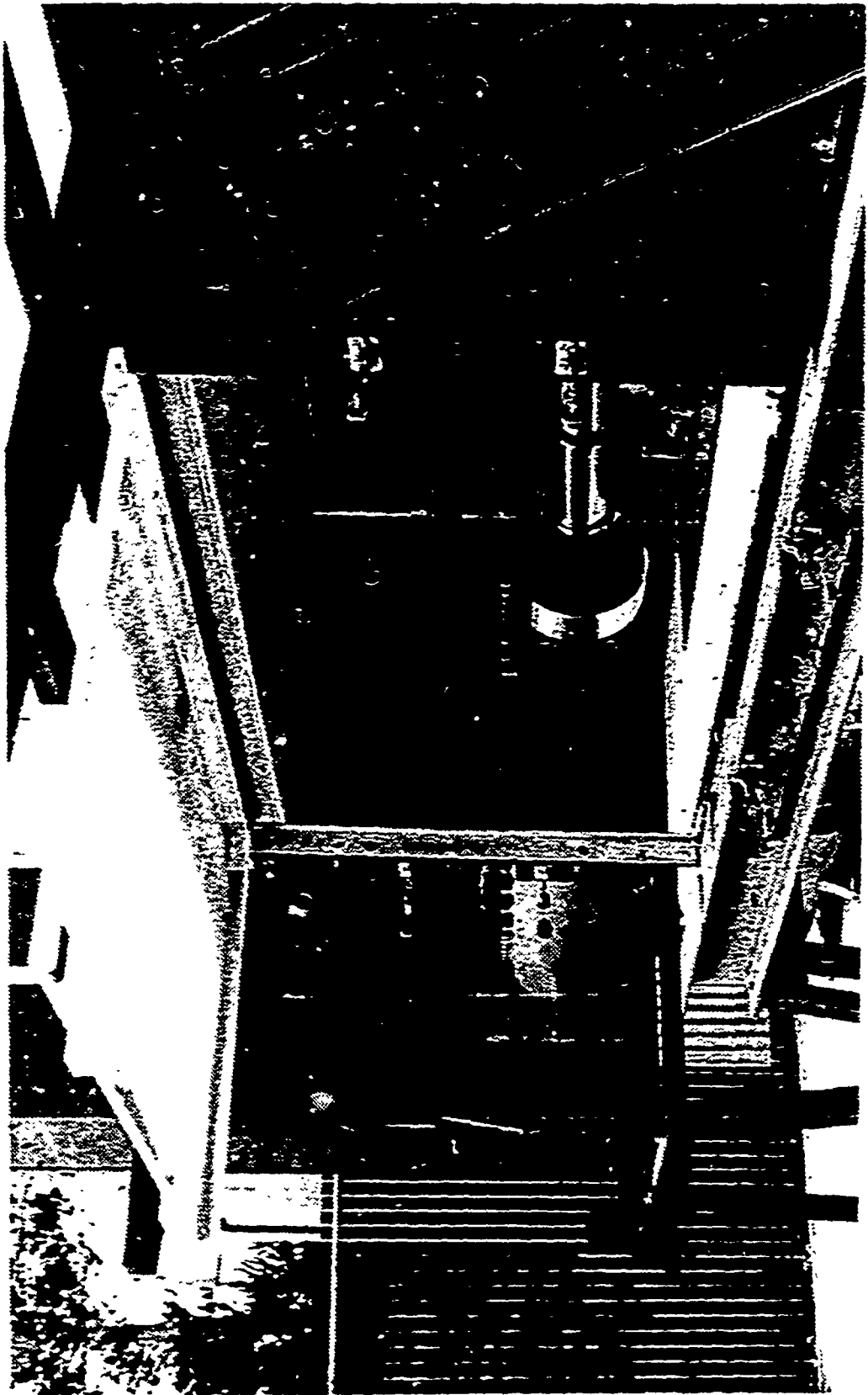


Fig. 1. Coll Test Section

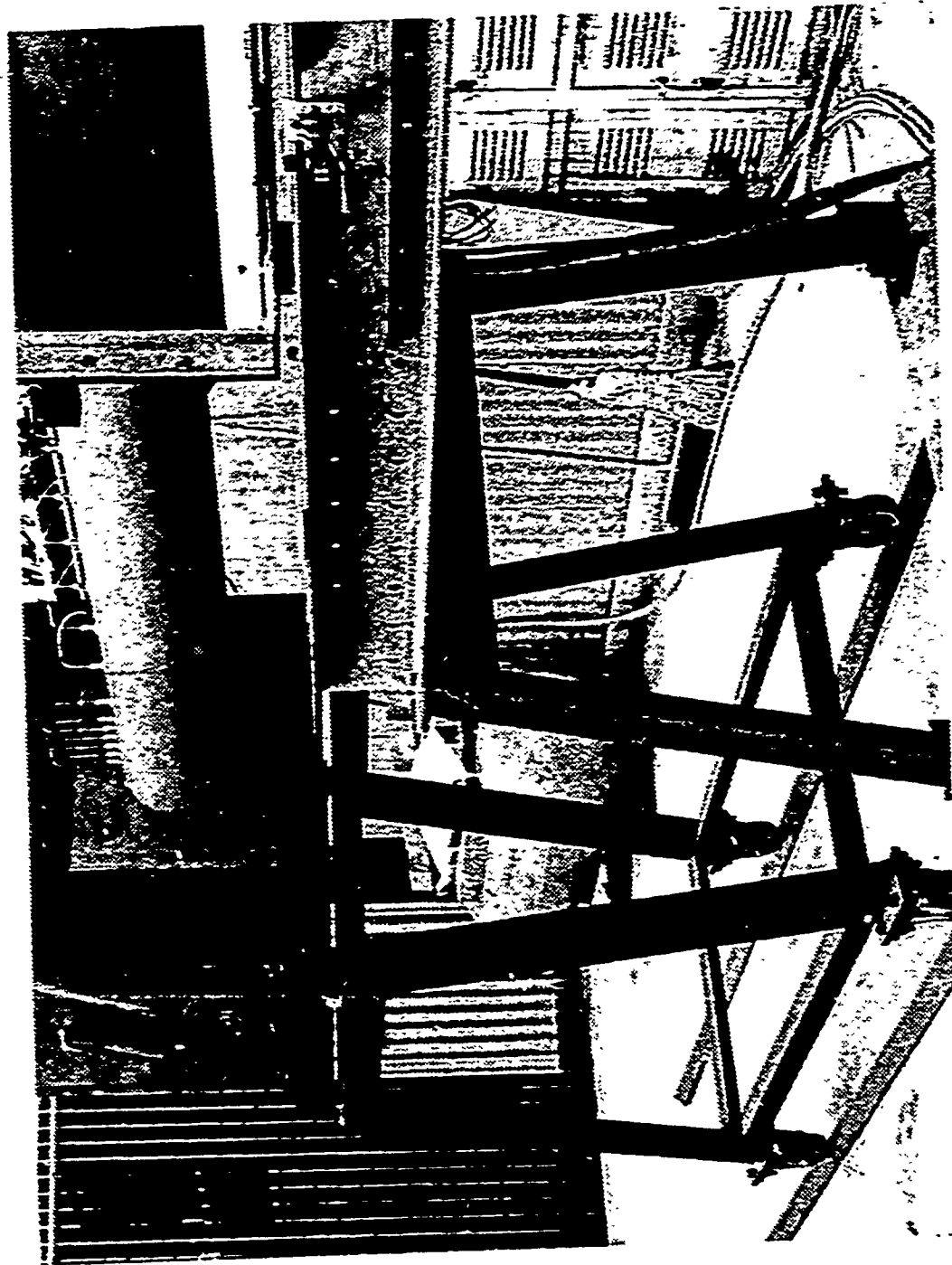


Fig. 2. Augmentor Tube and Stack Translation Apparatus

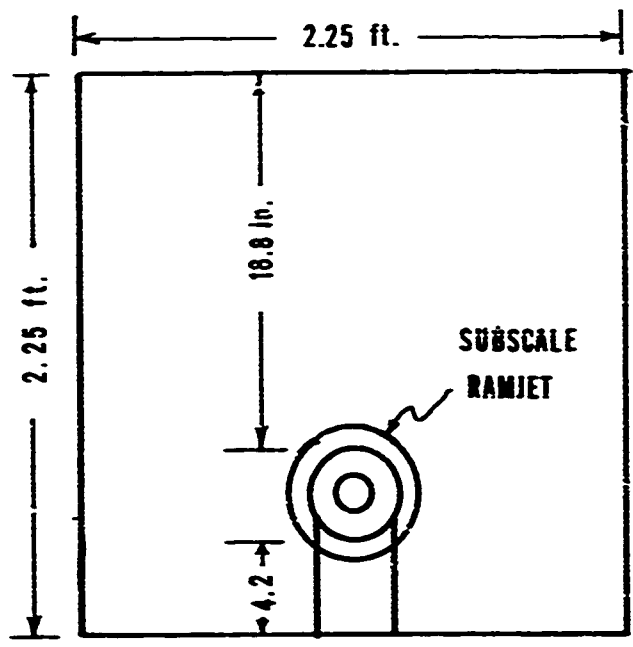


Fig. 3. End View of Test Section (Facing Upstream).

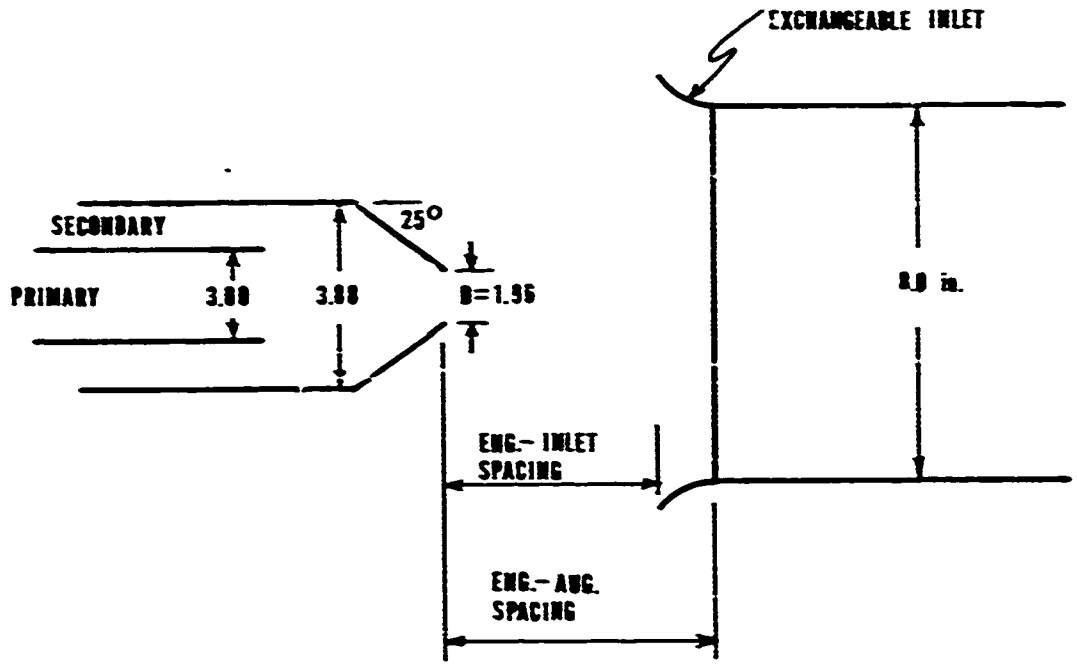


Fig. 4. Engine-Augmentor Interface Geometry.

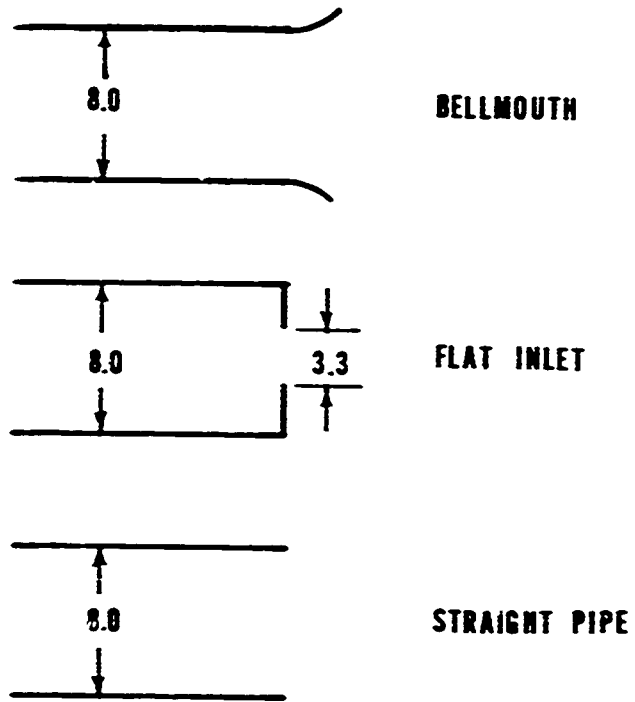


Fig. 5. Augmentor Inlet Variations.

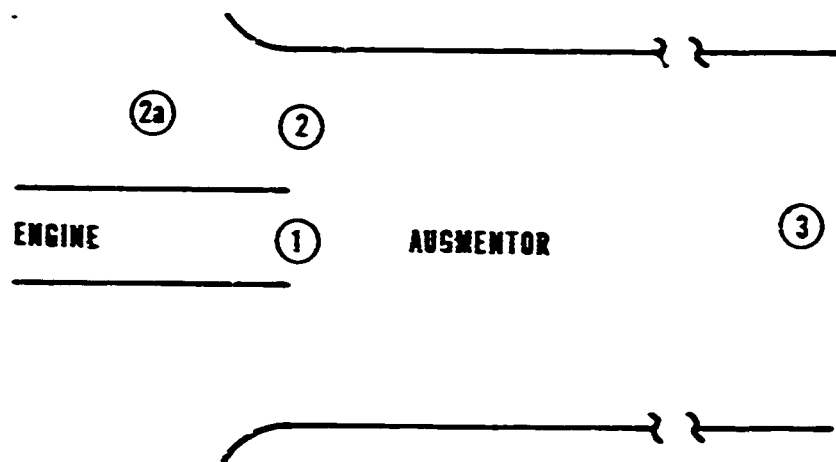


Fig. 6. One-Dimensional Model Geometry.

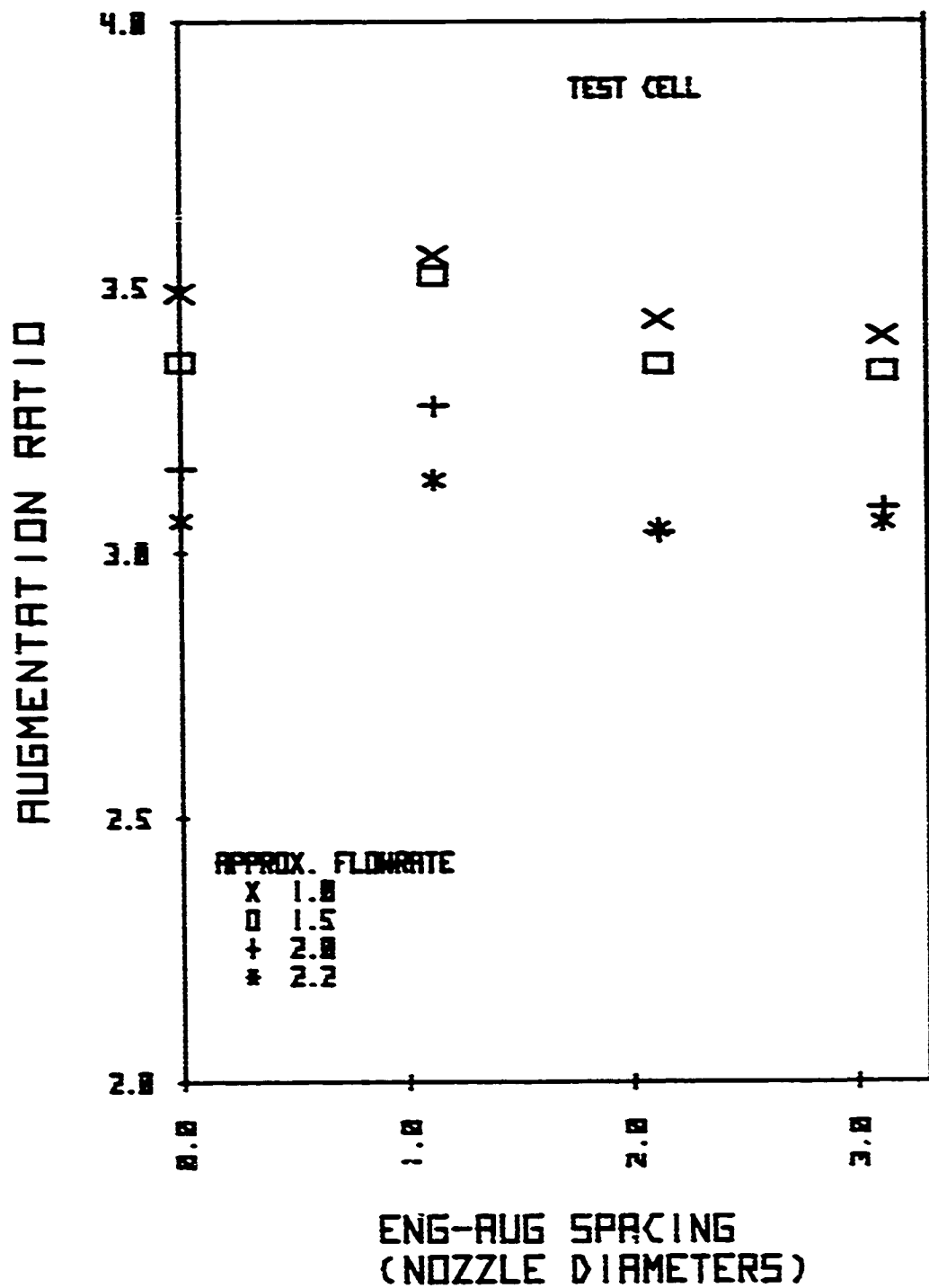


Fig. 7. Augmentation Ratio vs. Spacing (Test Cell).

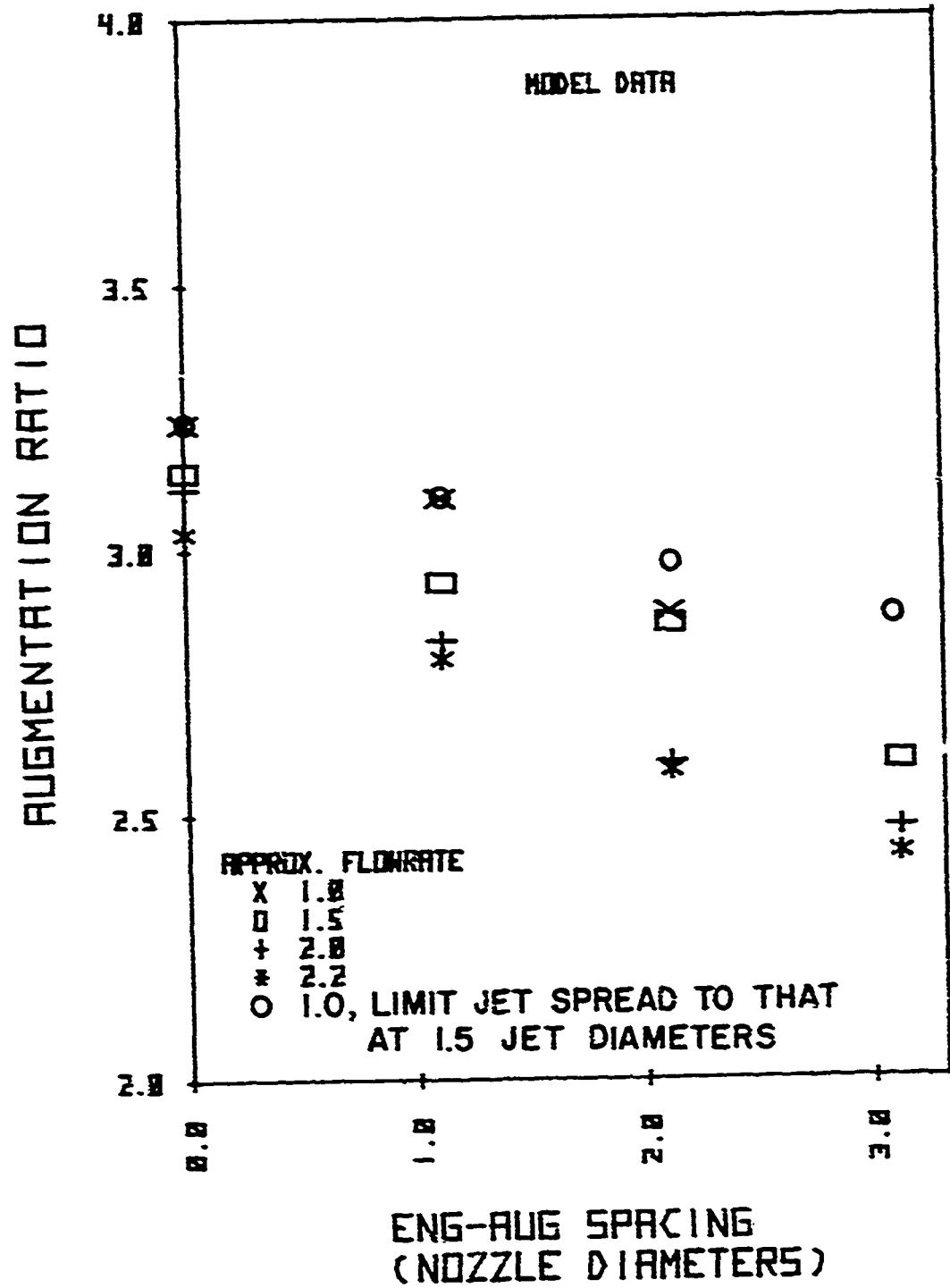


Fig. 8. Augmentation Ratio vs. Spacing (Model).

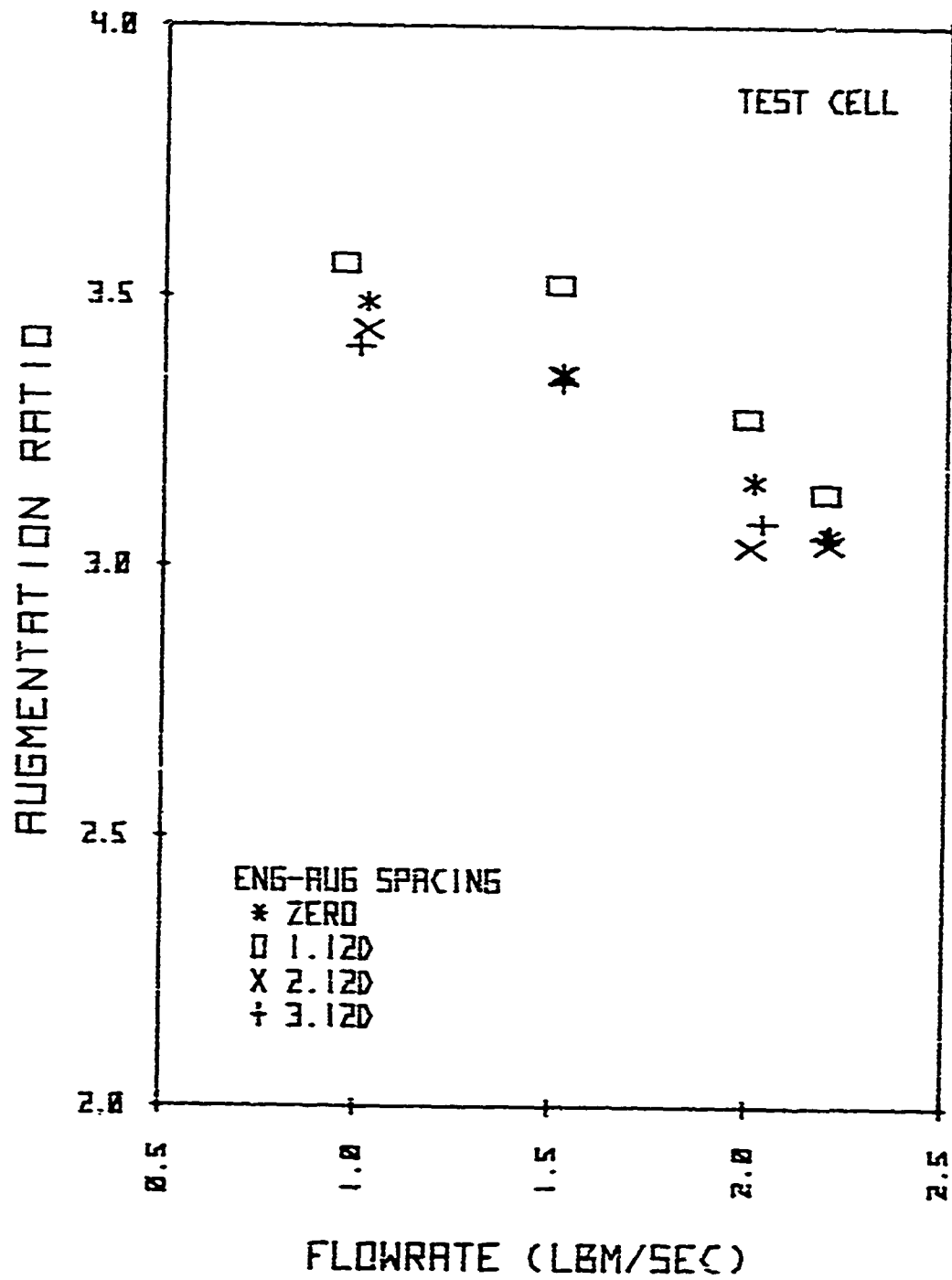


Fig. 9. Augmentation Ratio vs. Flow Rate (Test Cell).

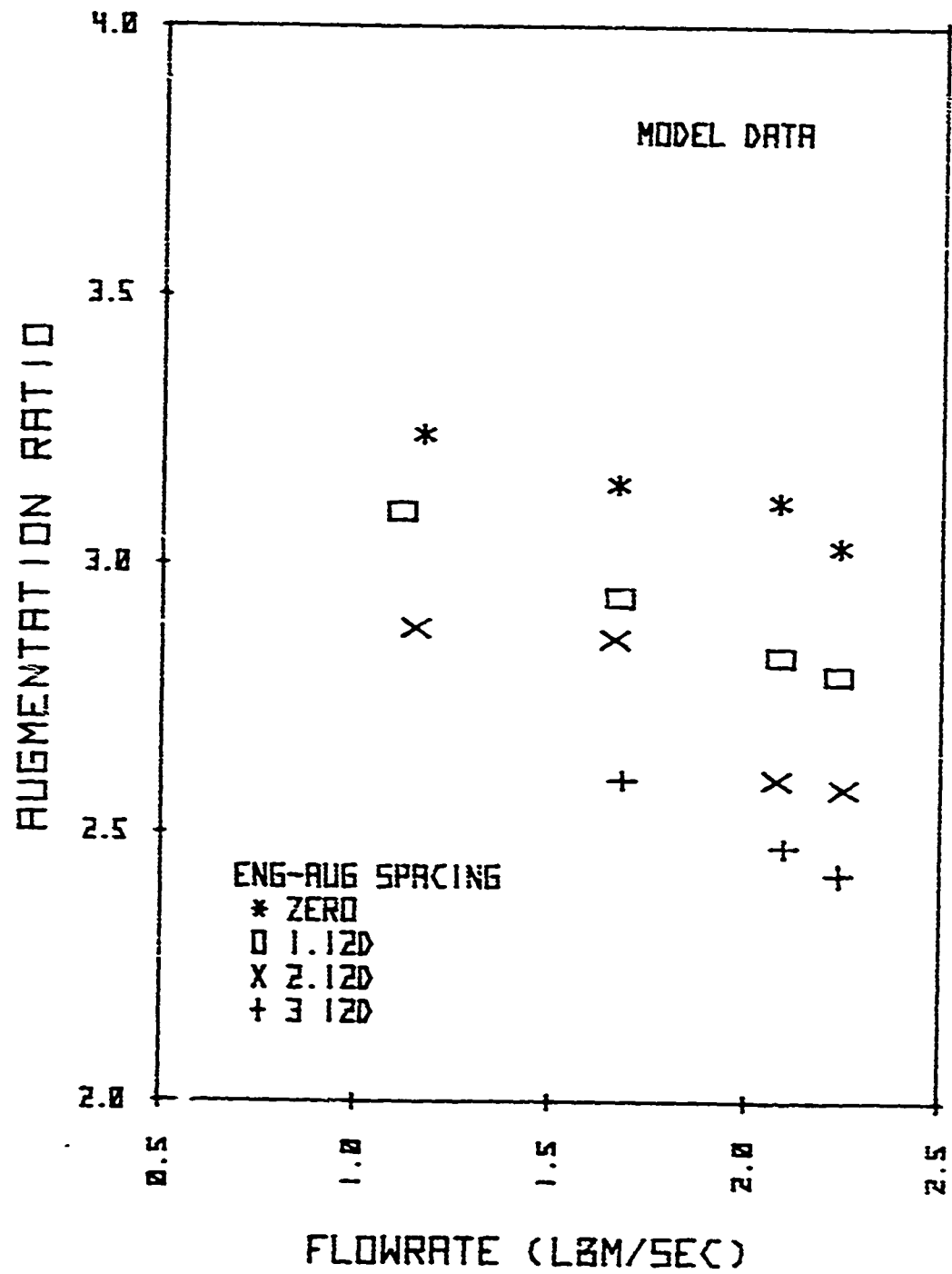


Fig. 10. Augmentation Ratio vs. Flow Rate (Model).

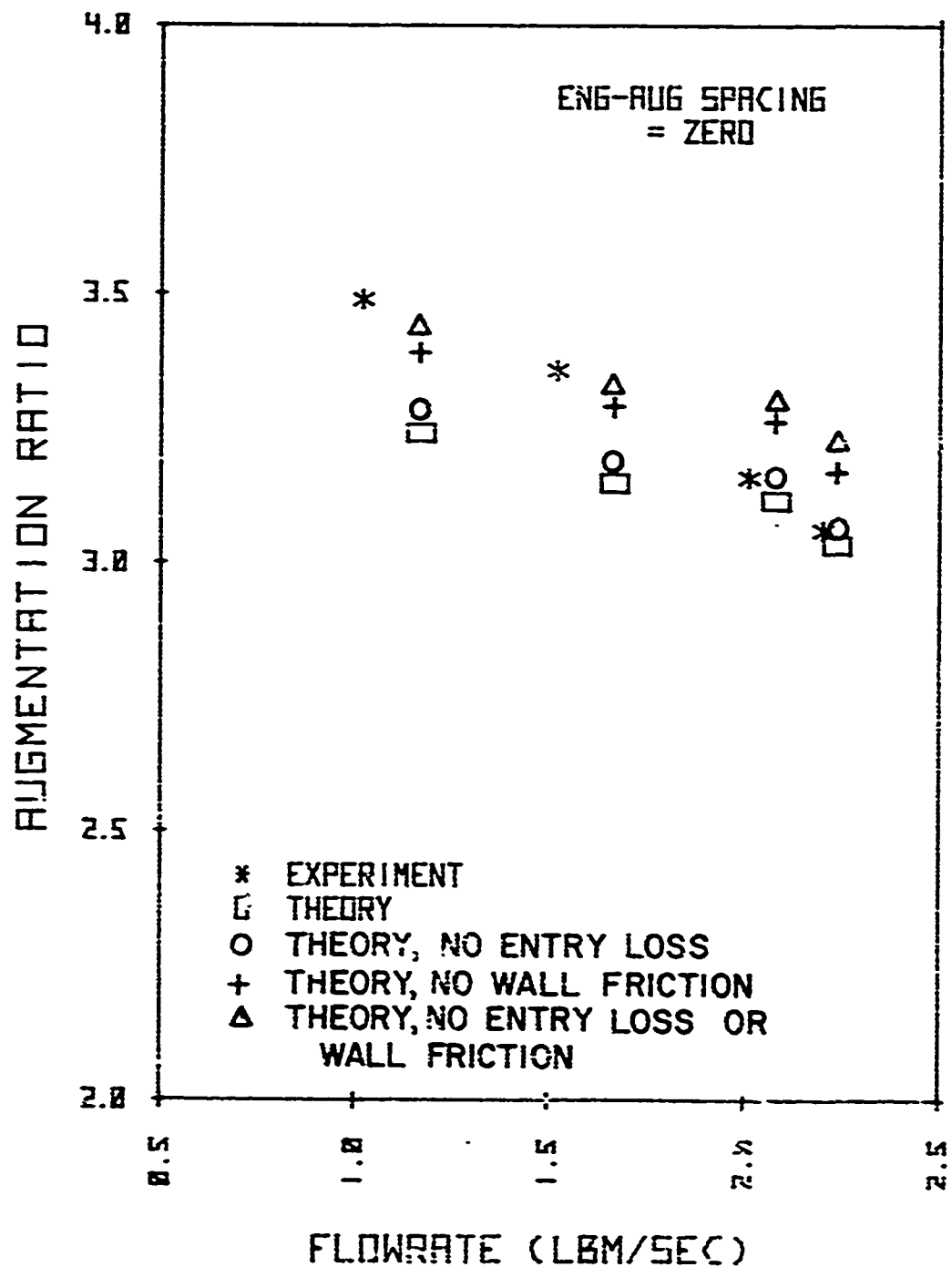


Fig. 13. Augmentation Ratio vs. Flow Rate, Zero Spacing

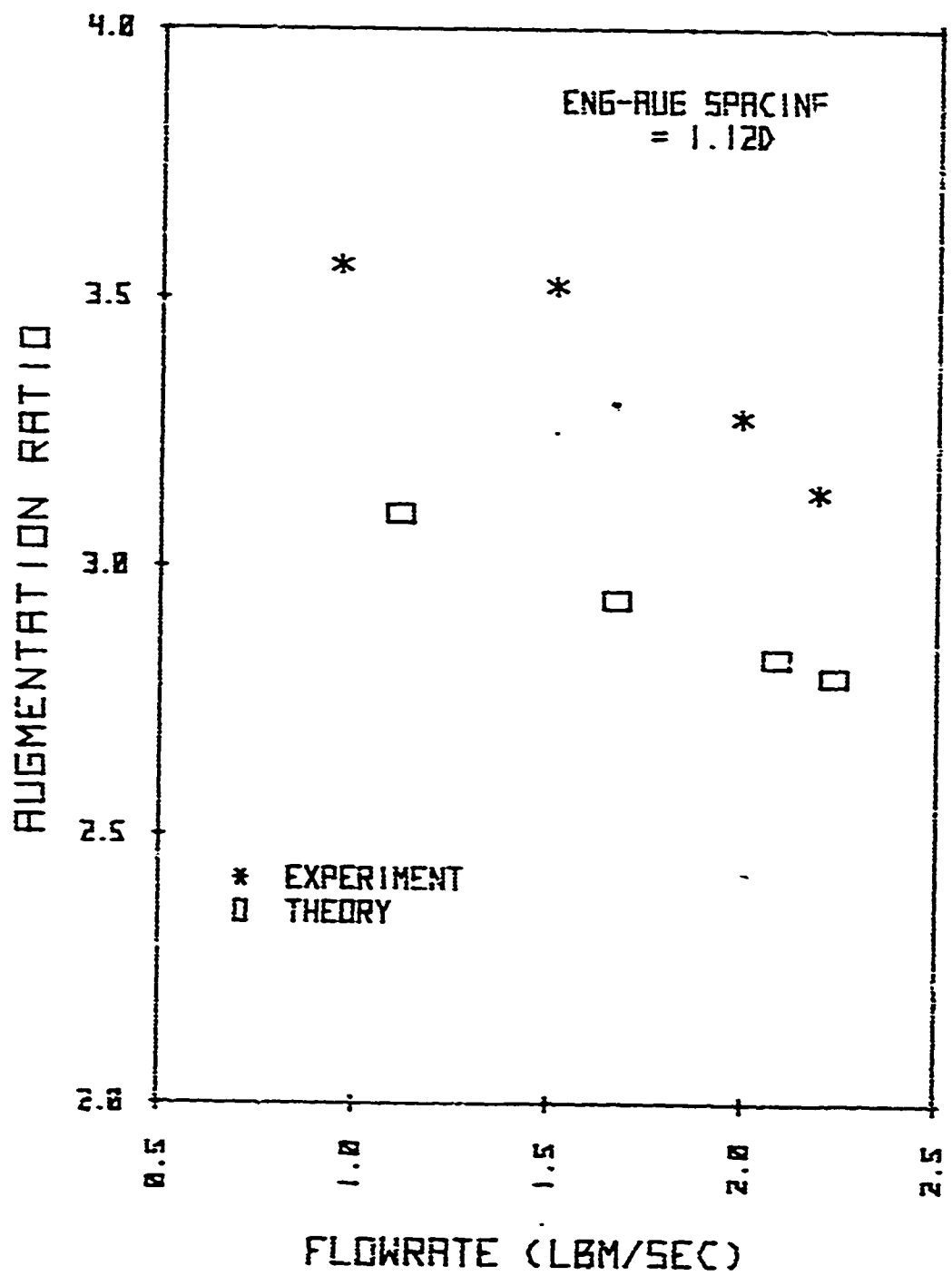


Fig. 12. Augmentation Ratio vs. Flow Rate, 1.12D Spacing

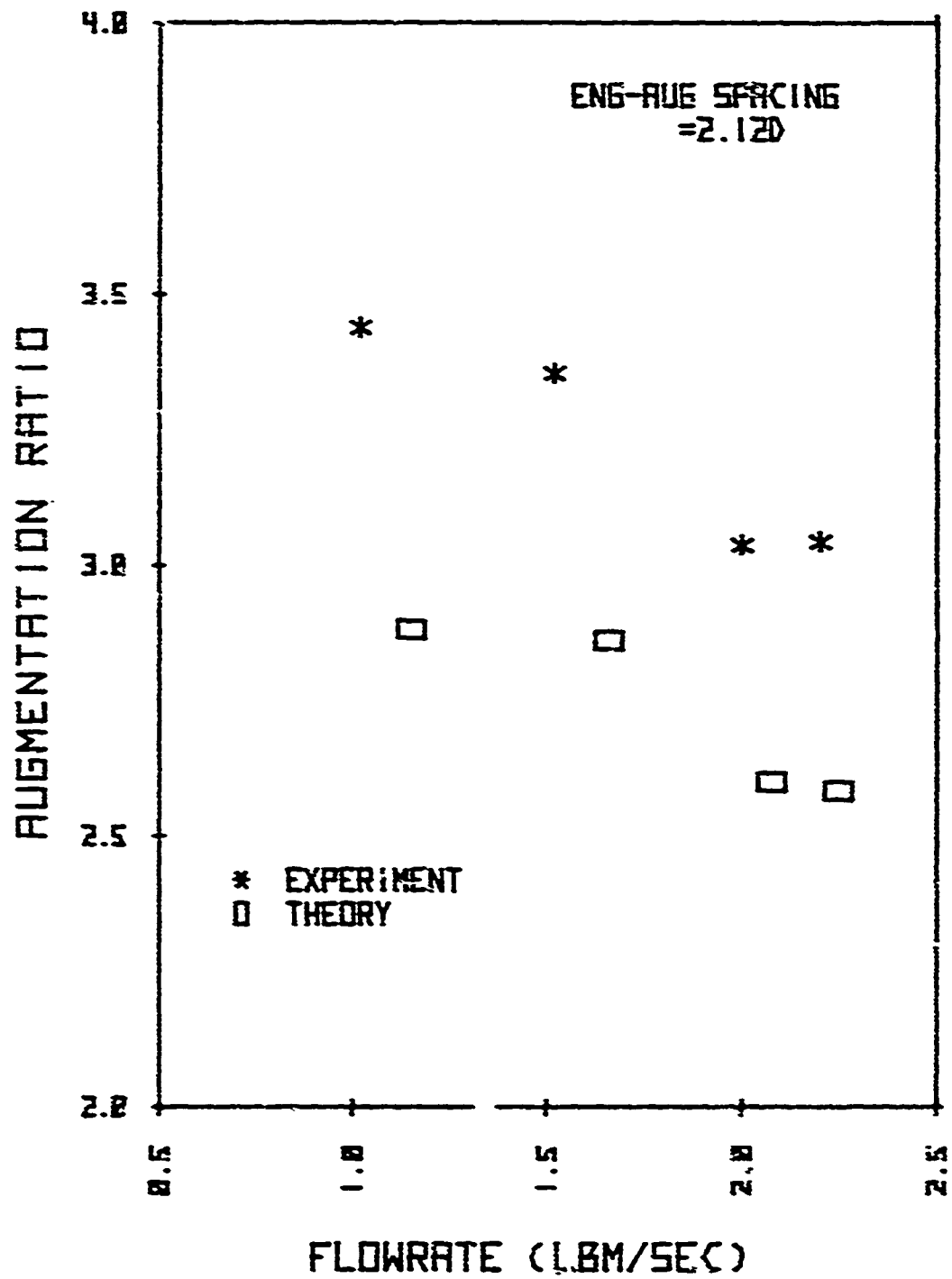


Fig. 13. Augmentation Ratio vs. Flow Rate, 3.12D Spacing

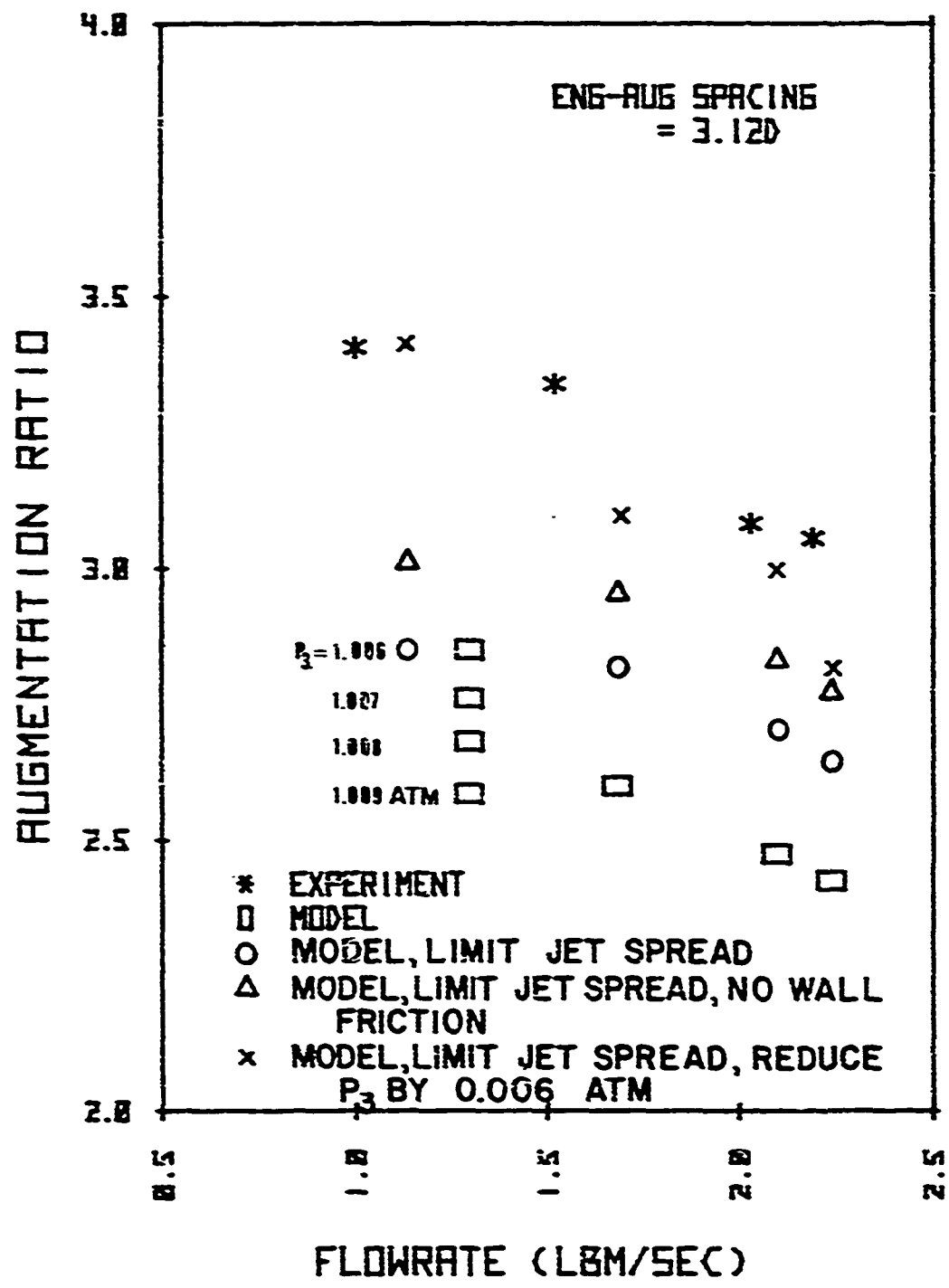


Fig. 14. Augmentation Ratio vs. Flow Rate, 3.12D Spacing

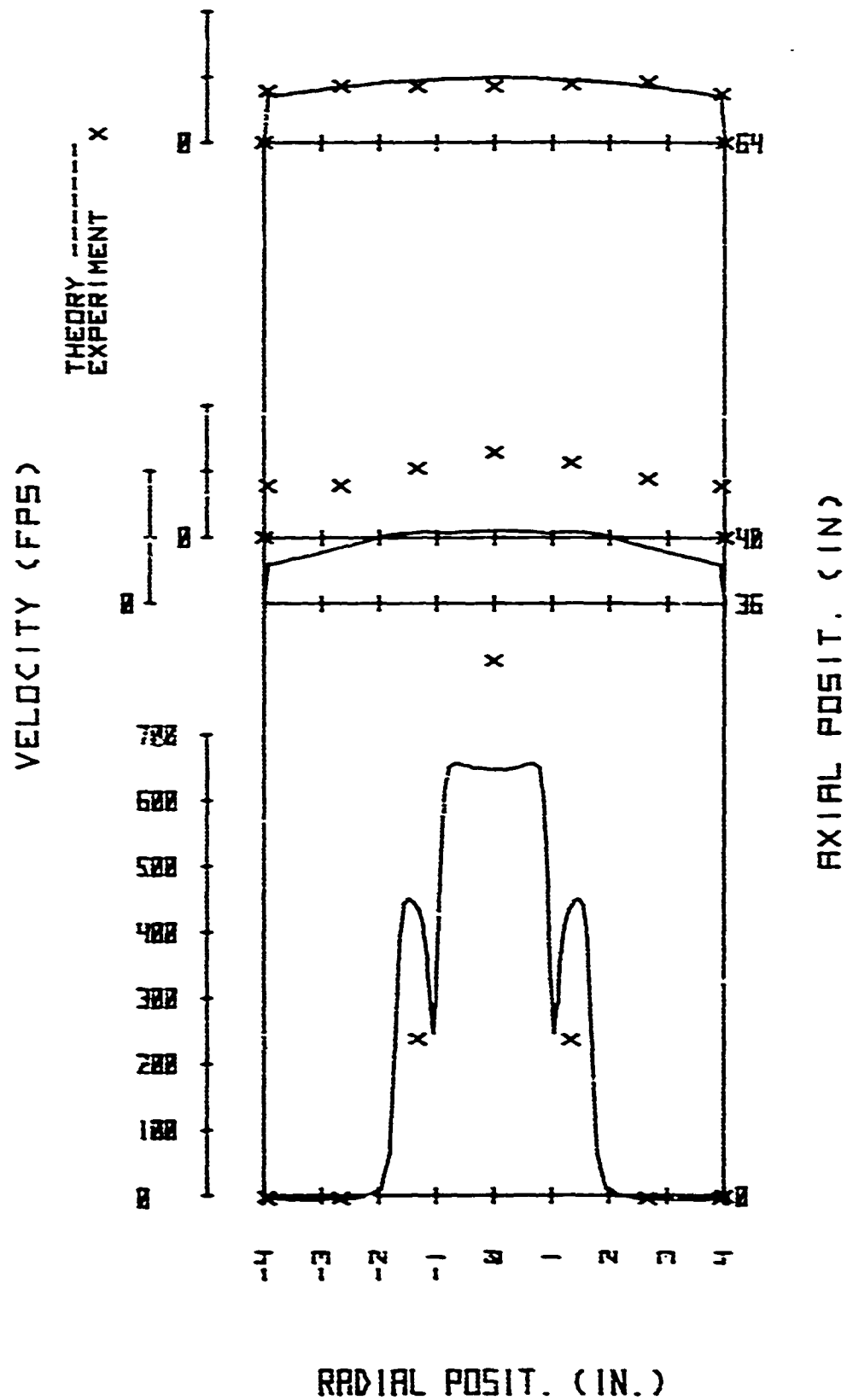


Fig. 15. Augmentor Velocity Profiles; Flow Rate = 1.0; Spacing = 0; Augmentation Ratio = 1.26; Cold Flow.

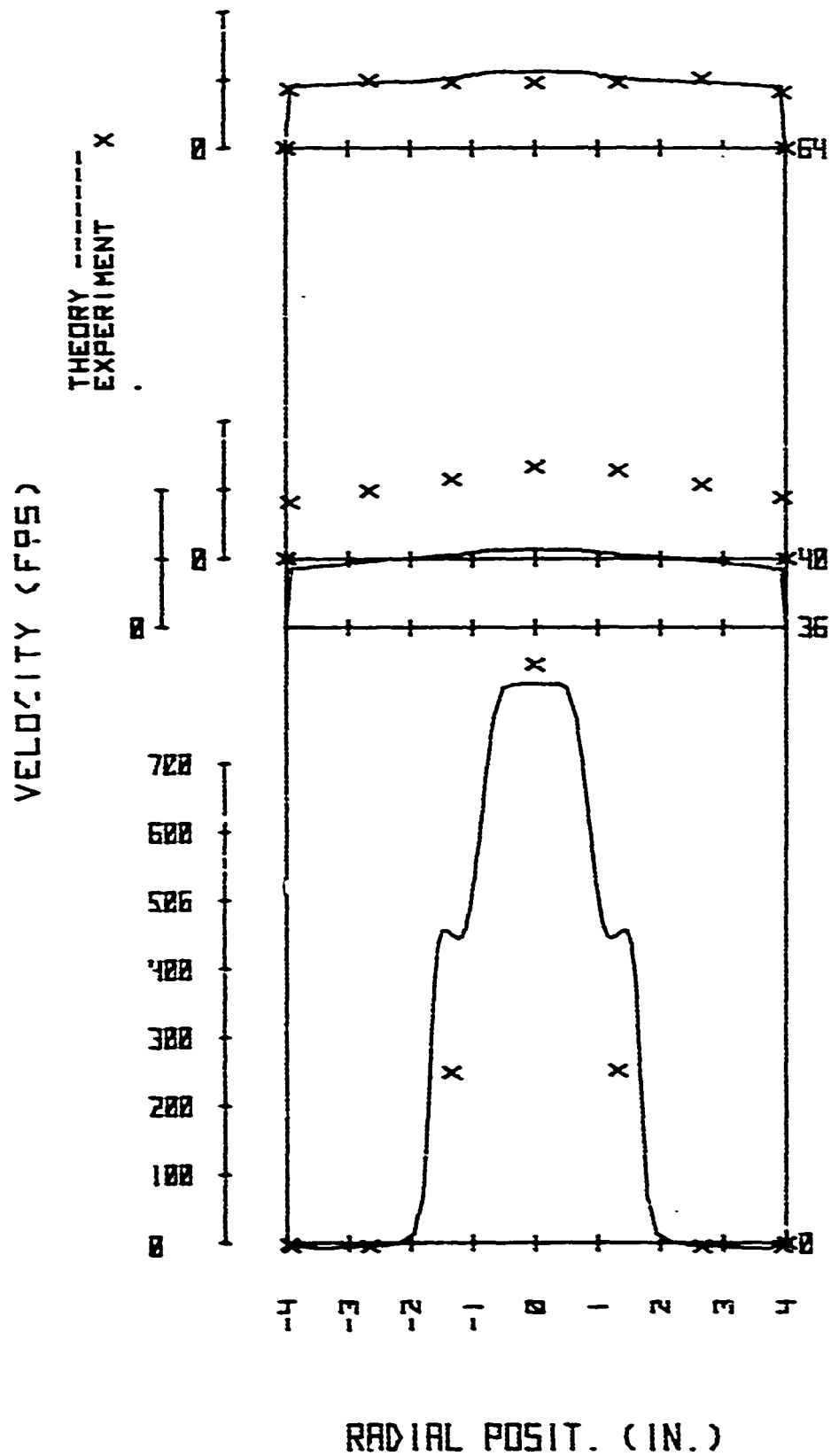
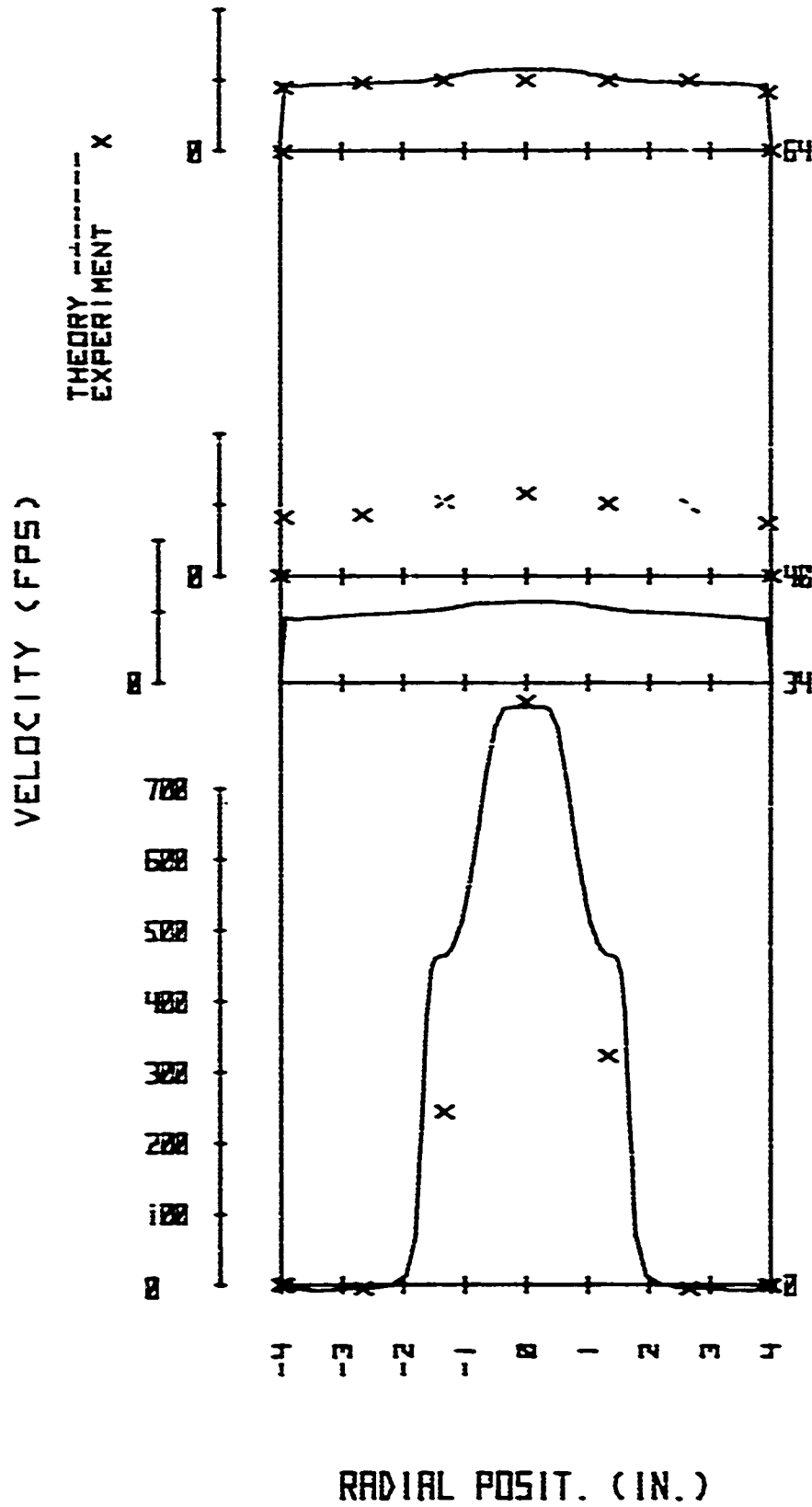
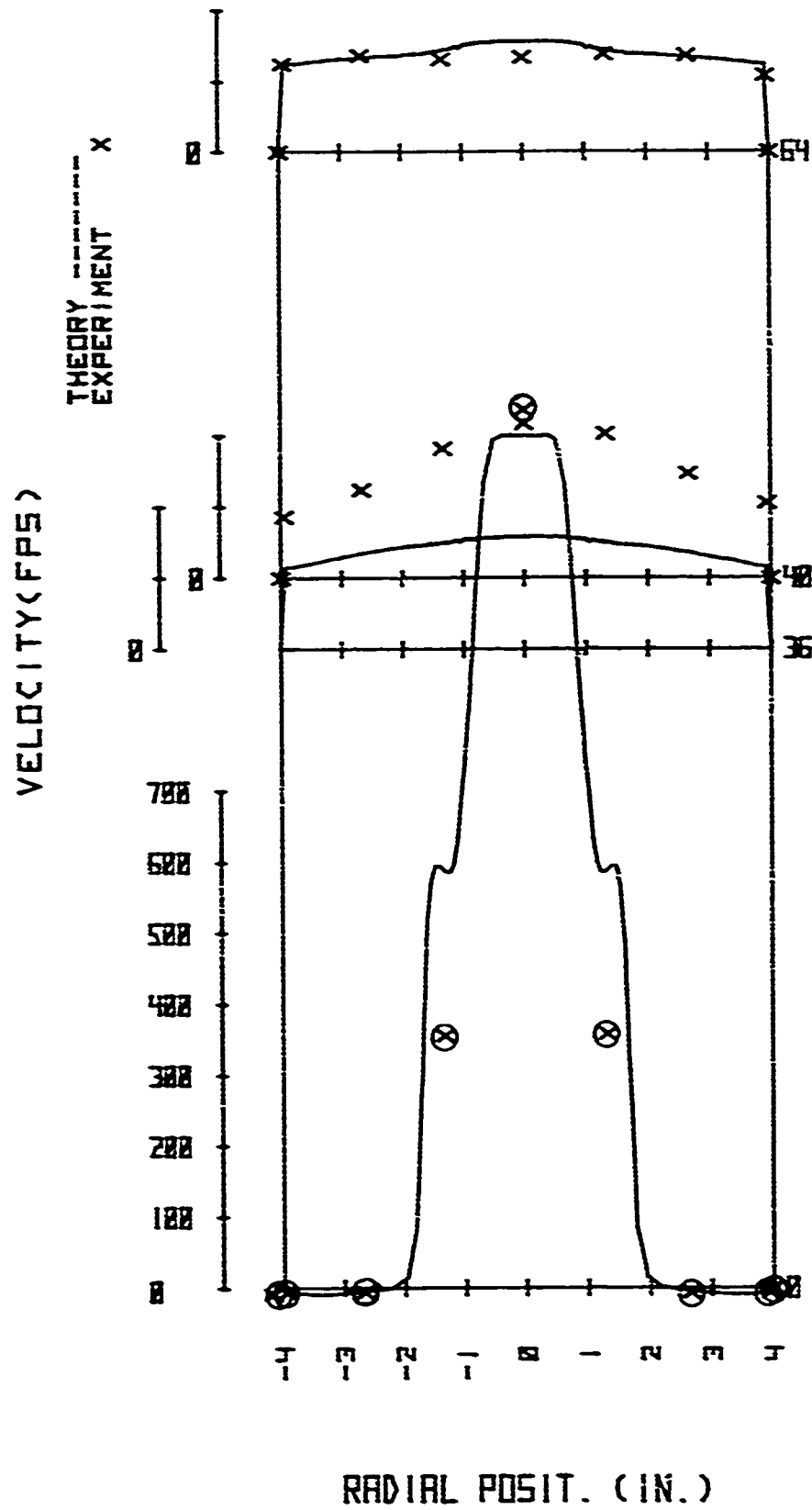


Fig. 16. Augmentor Velocity Profiles: Flow Rate = 1.0; Spacing = 1
Nozzle Diameter; Augmentation Ratio = 1.52; Cold Flow.



AXIAL POSIT. (IN)

Fig. 17. Augmentor Velocity Profiles; Flow Rate = .99; Spacing = 2
Nozzle Diameters; Augmentation Ratio = 1.55; Cold Flow.



AXIAL POSIT. (IN)

Fig. 18. Augmentor Velocity Profiles: Flow Rate = 1.52; Spacing = 1
Nozzle Diameter; Augmentation Ratio = 1.29; Cold Flow.

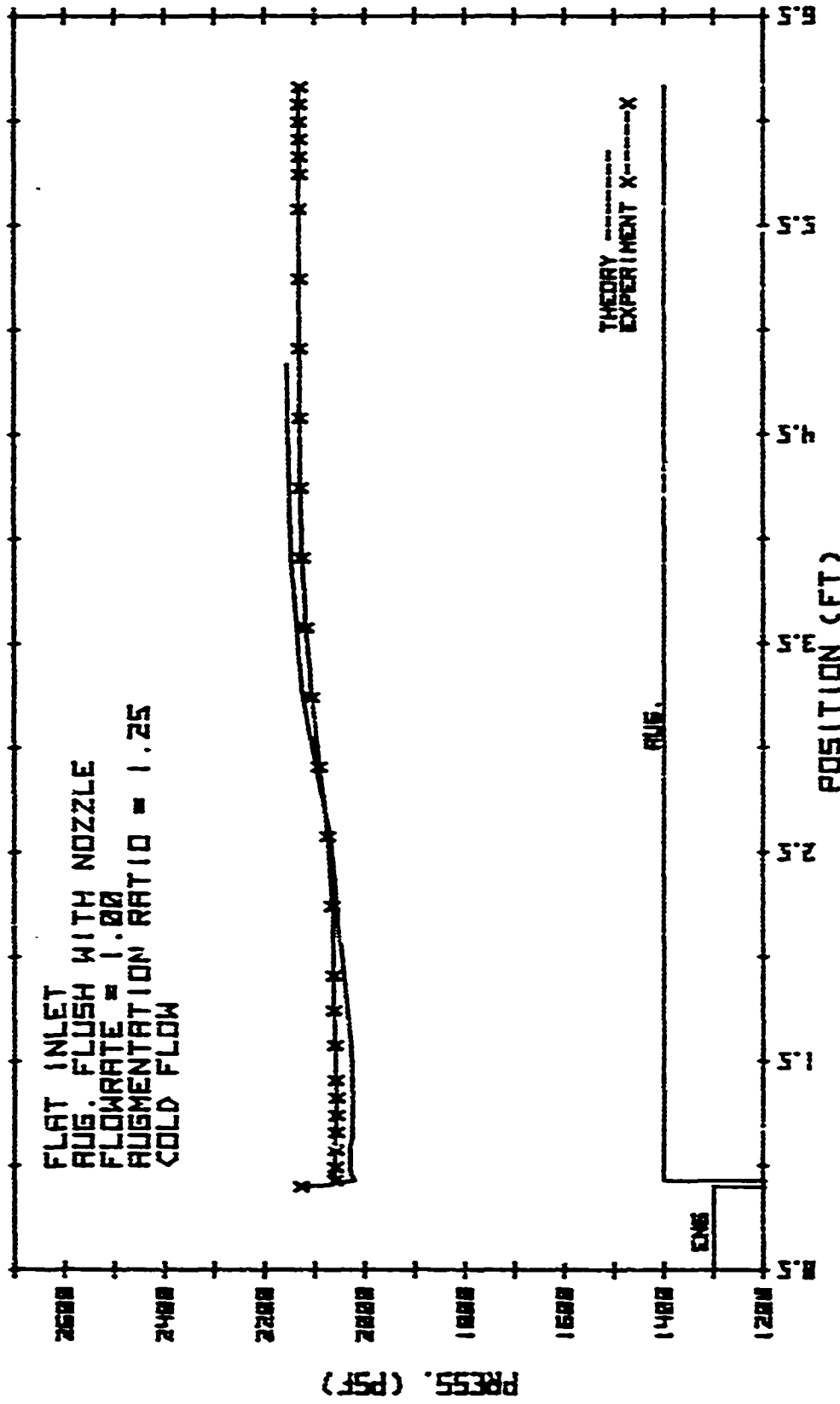


Fig. 19. Augmentor Pressure Profile, Flat Inlet, Zero Spacing

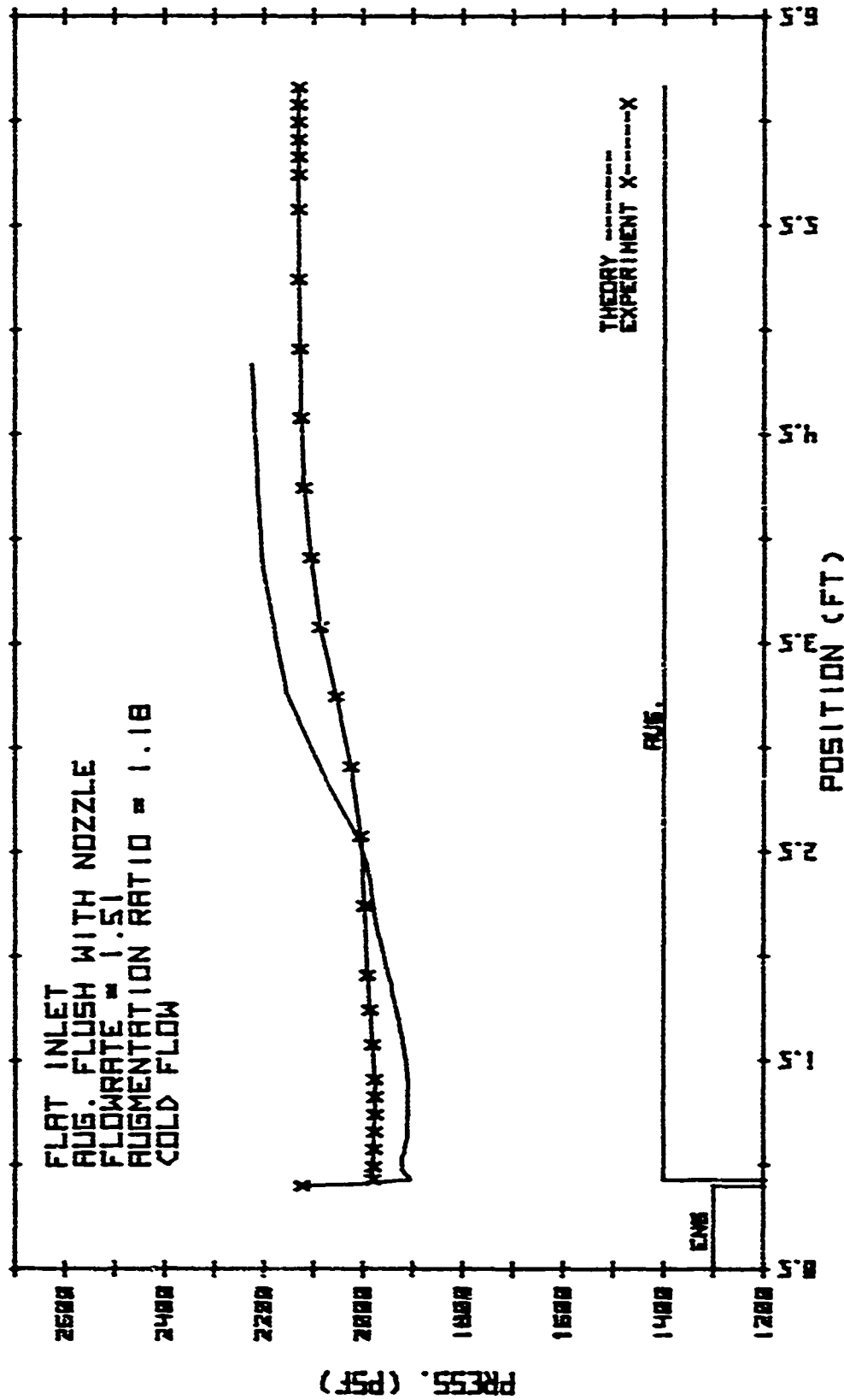


Fig. 20. Augmentor Pressure Profile, Flat Inlet, Zero Spacing

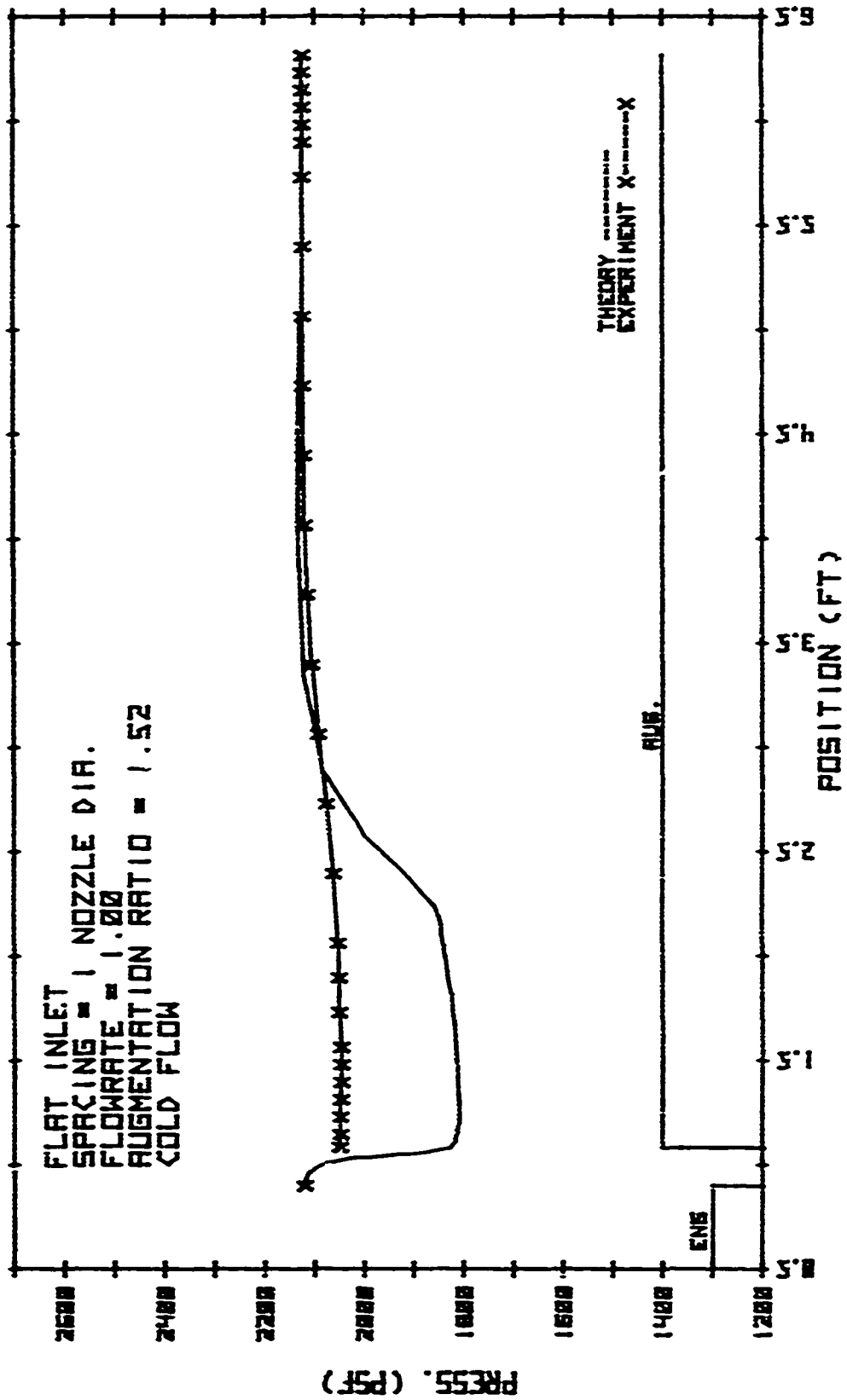


Fig. 21. Augmentor Pressure Profile, Flat Inlet, 1-D Spacing

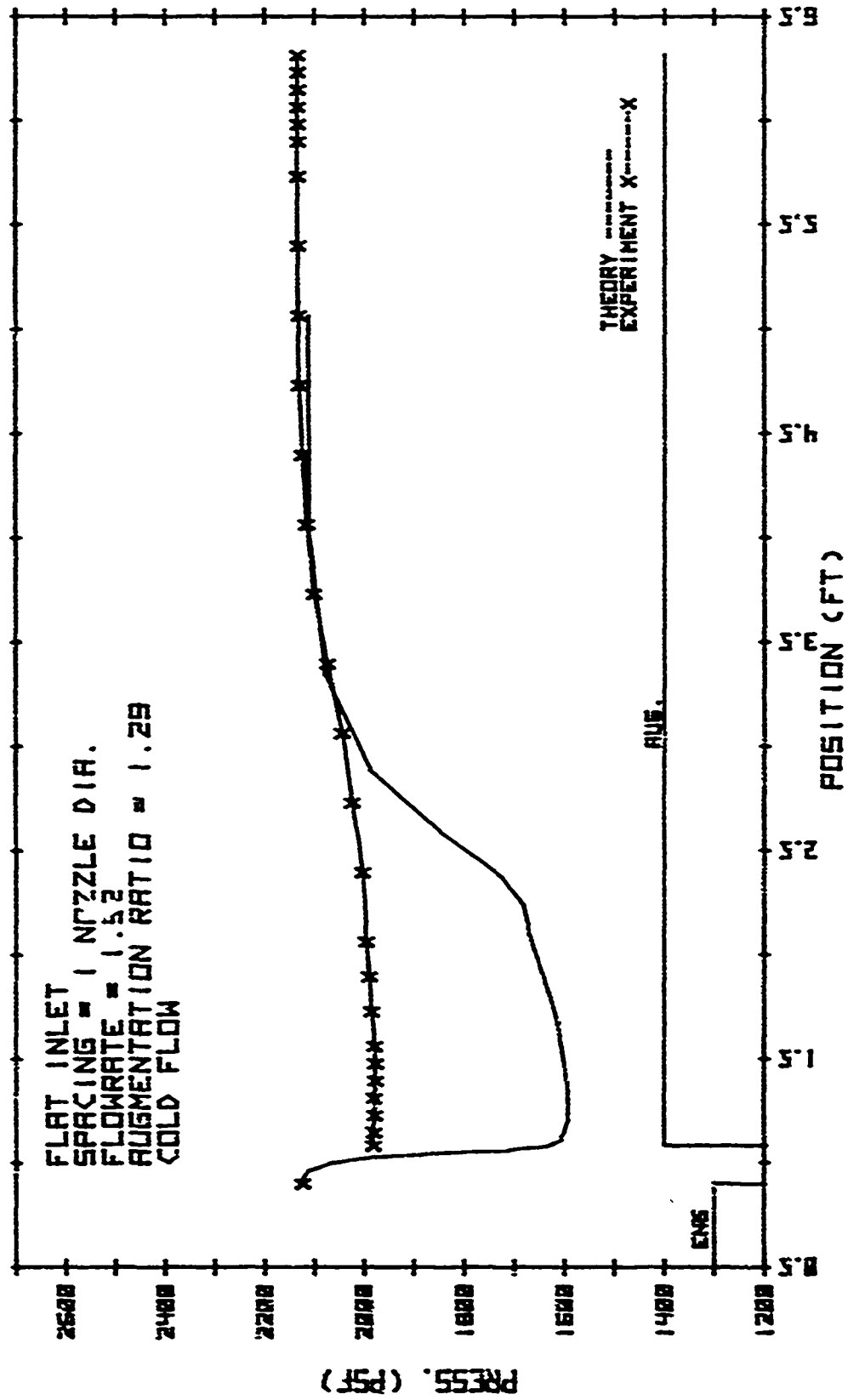


Fig. 22. Augmentor Pressure Profile, Flat Inlet, 1-D Sacing

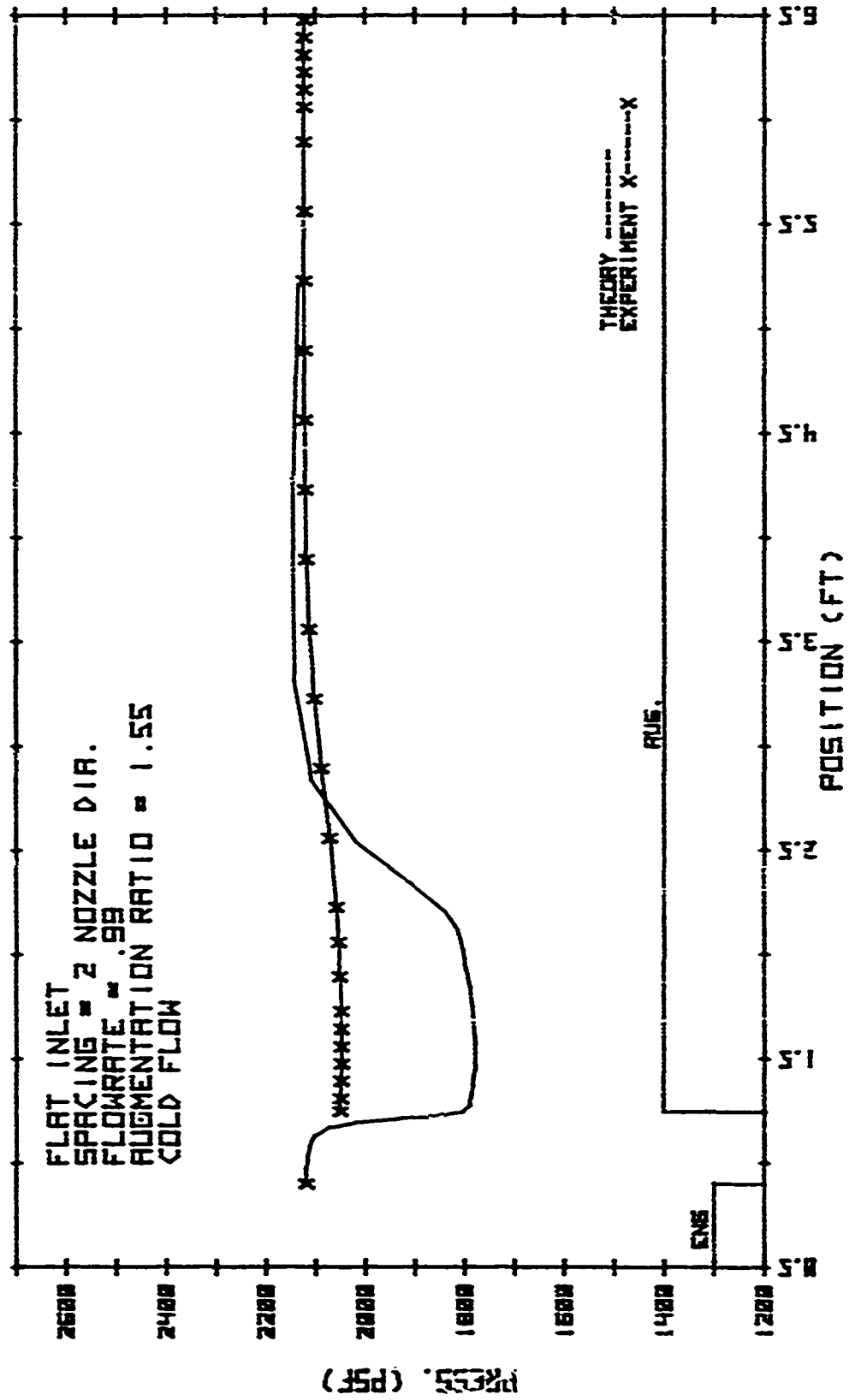


Fig. 23. Augmentor Pressure Profile, Flat Inlet, 2-D Spacing

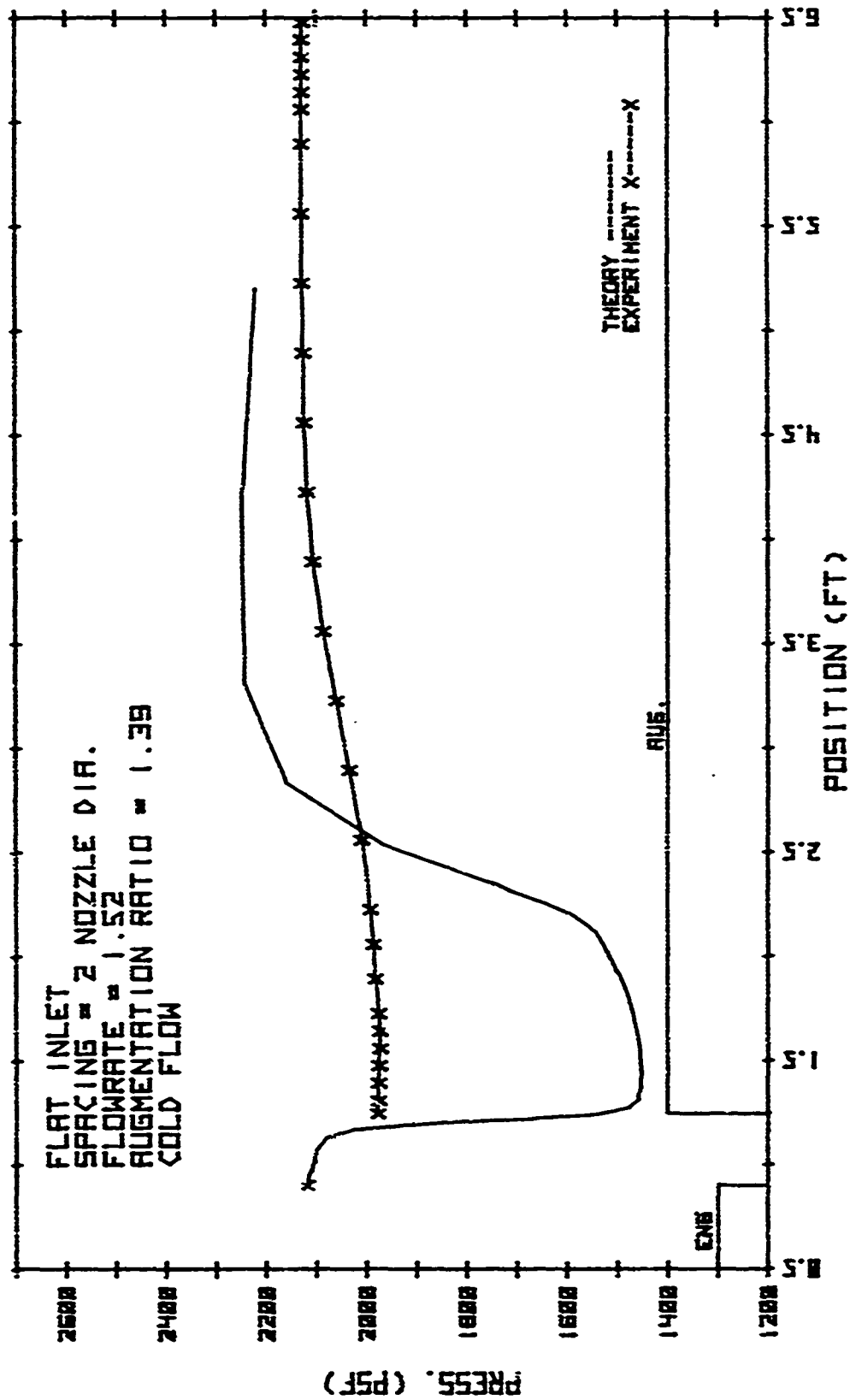


Fig. 24. Augmentor Pressure Profile, Flat Inlet, 2-D Spacing

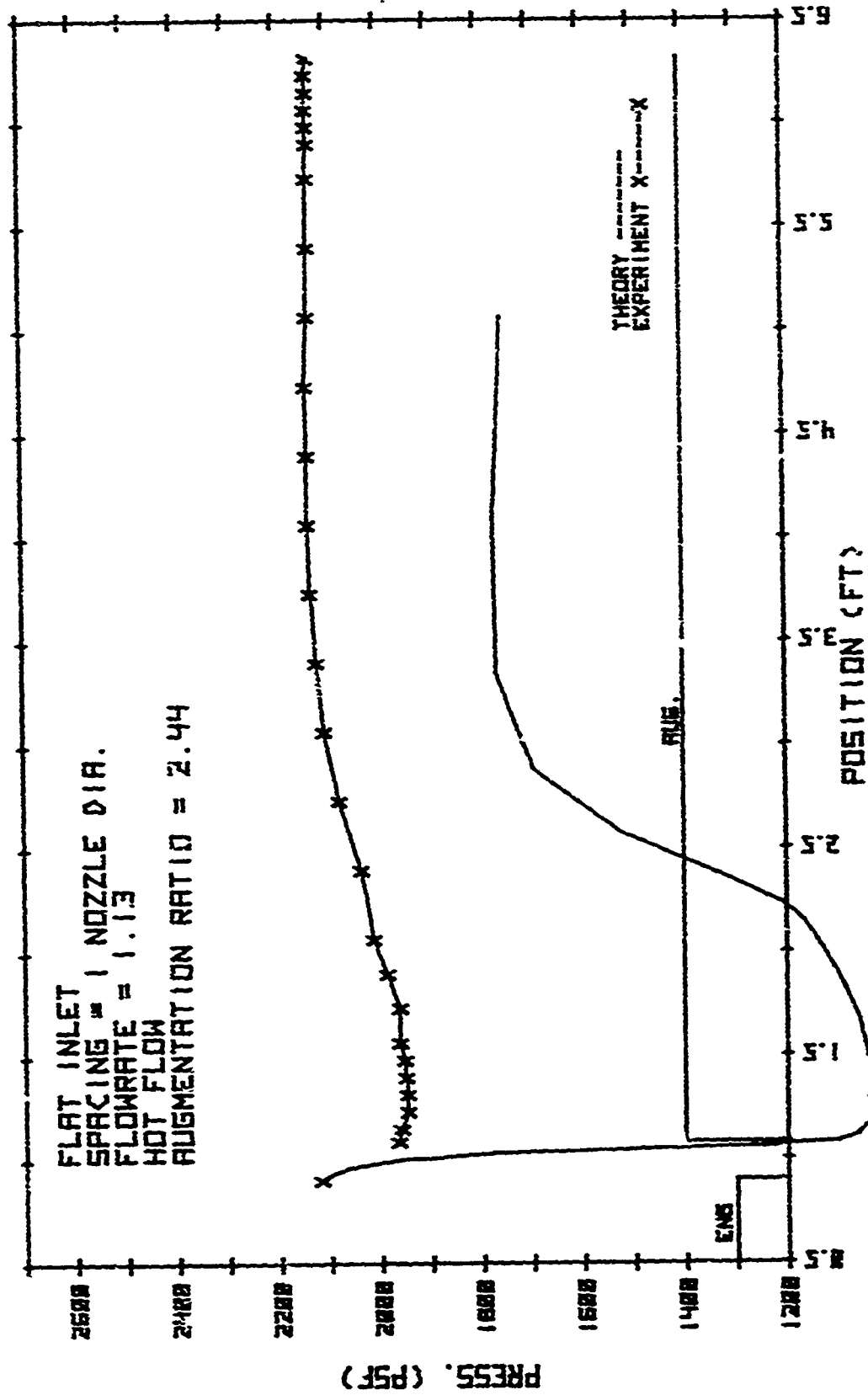


Fig. 25. Augmentor Pressure Profile, Flat Inlet, 1-D Spacing, Hot Flow

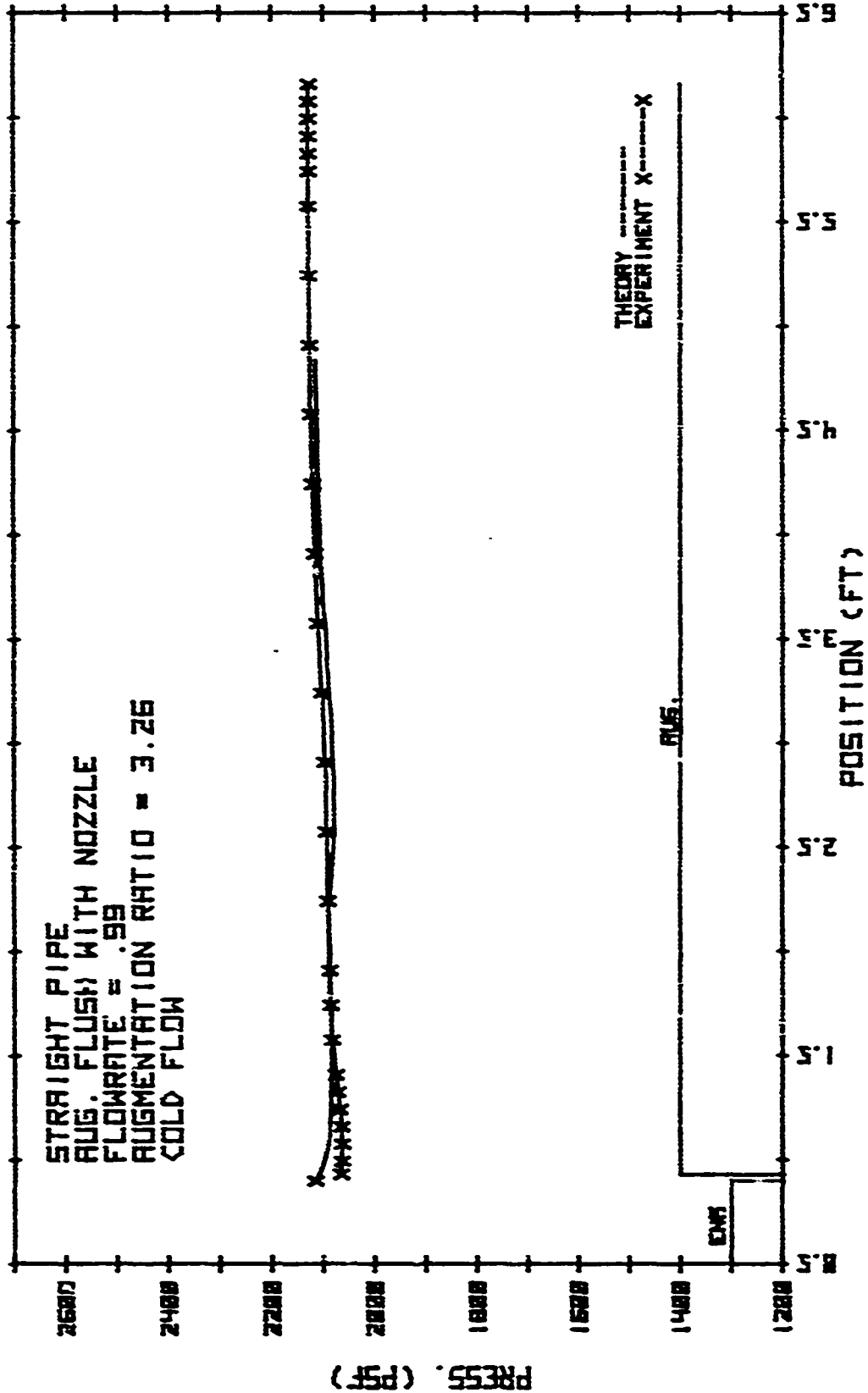


Fig. 26. Augmentor Pressure Profile, Straight Inlet, Zero Spacing

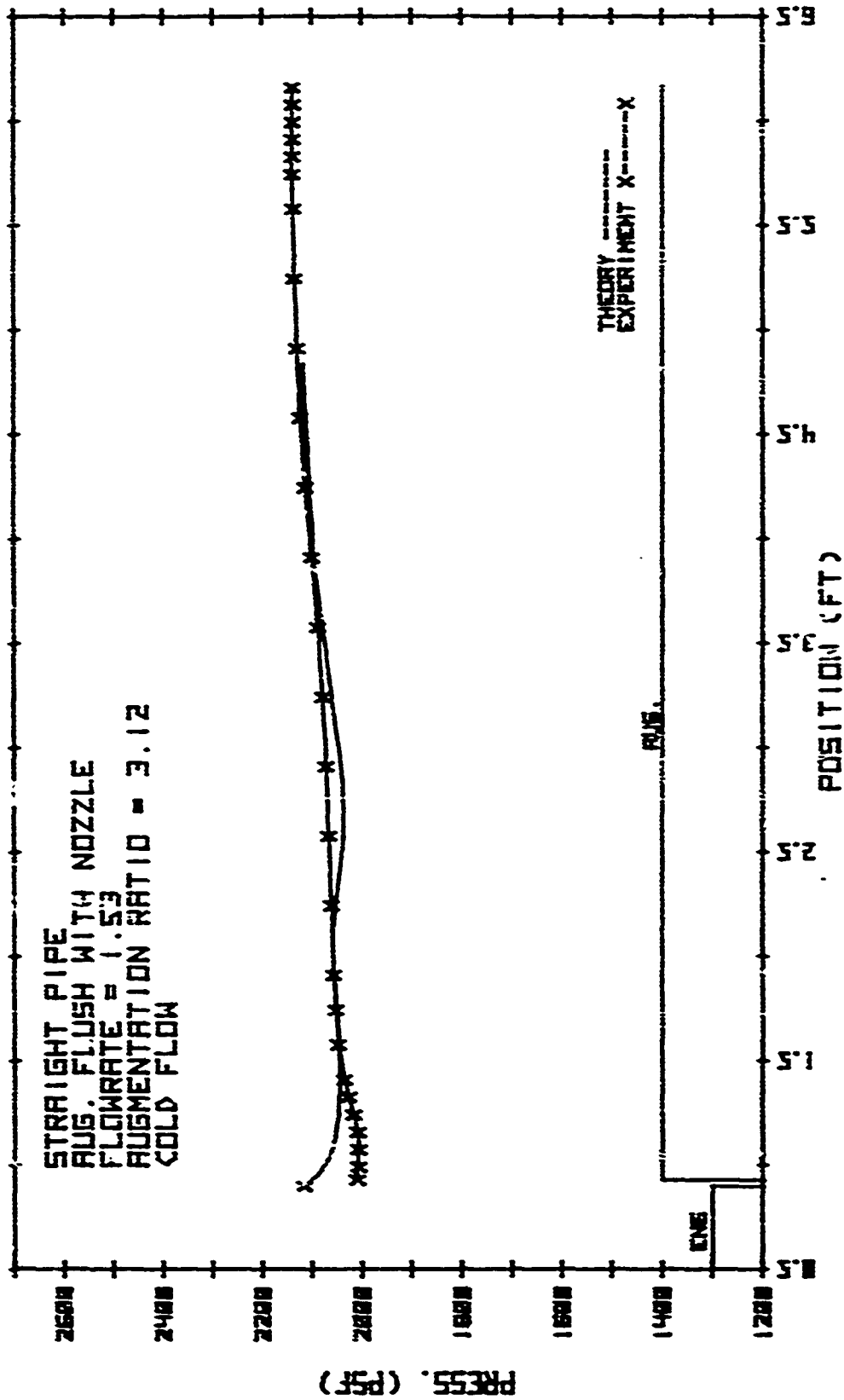


Fig. 27. Augmentor Pressure Profile, Straight Inlet, Zero Spacing

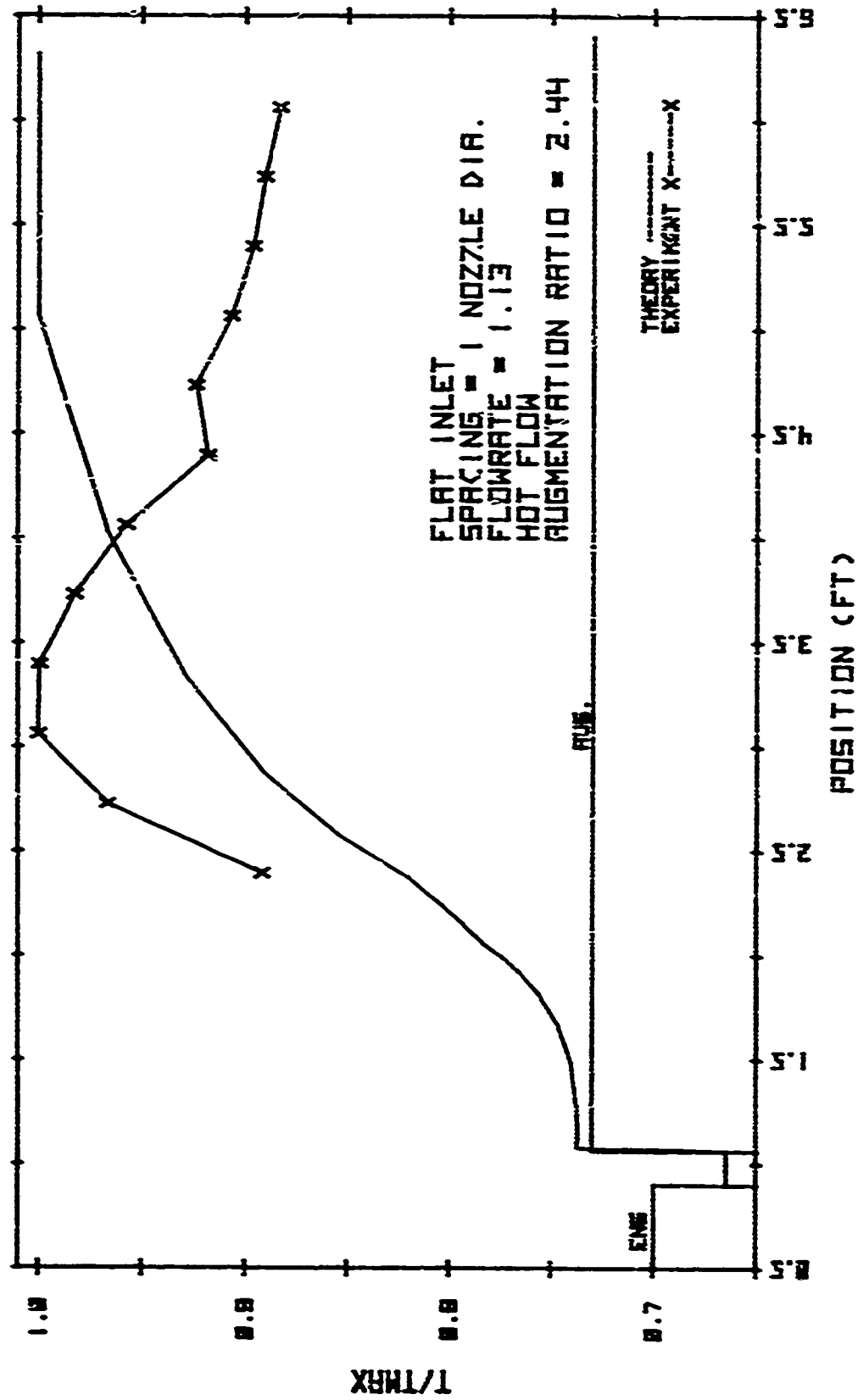


Fig. 28. Augmentor Temperature Profile, Flat Inlet, 1-D Spacing

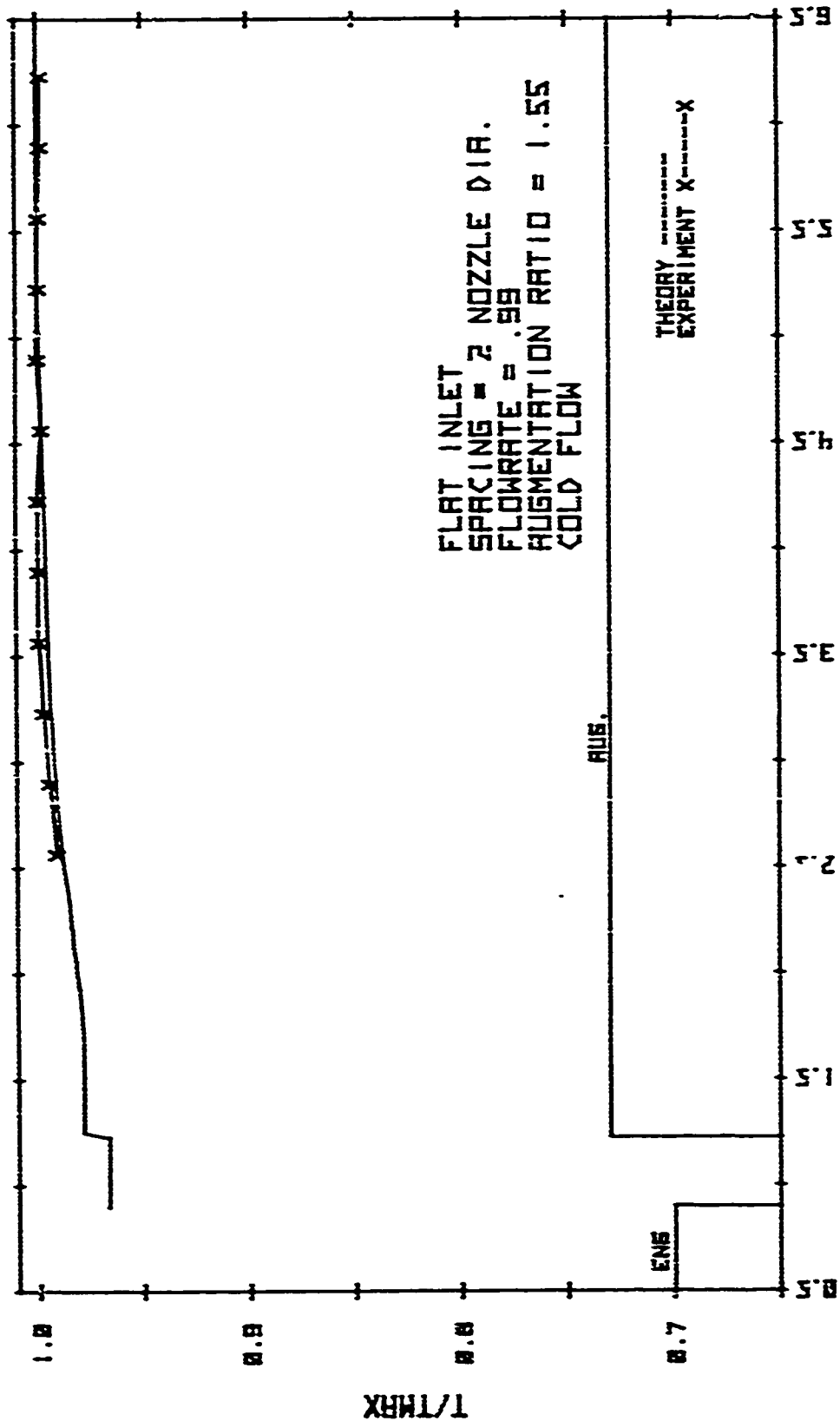


Fig. 29. Augmentor Temperature Profile, Flat Inlet, 2-D Spacing

LIST OF REFERENCES

1. Fluidyne Engineering Corporation Report for the Naval Facilities Engineering Command, Aerodynamic and Accoustic Tests of a 1/15 Scale Model Dry Cooled-Jet Aircraft Runup Noise Suppression System, by J. L. Grunnat and I. L. Ver., October 1975.
2. American Institute of Aeronautics and Astronautics Paper No. 75-1328, Air Cooled Ground Noise Suppressor for After-burning Engines Using the Coanda Effect, by M. D. Nelson, G. J. Kass, R. E. Ballard, and D. L. Armstrong,
3. Advisory Group for Aerospace Research and Development Report 125, Pollution Control of Airport Engine Test Facilities, by D. L. Bailey, P. W. Tower, and A. E. Fuhs, April 1973.
4. United Aircraft Research Laboratories, Air Force Weapons Laboratory Report AFWL-TR-73-18, Analysis of Jet Engine Test Cell Pollution Abatement Methods by F. L. Robson, A. S. Kesten, R. D. Lassard, May 1973.
5. Ellin, C. R. and Pucci, P. F., Model Tests of Multiple Nozzle Exhaust Gas Turbine Powered Ships, M.E. Thesis, Naval Postgraduate School, Monterey, California, June 1977.
6. Bailey, D. L., An Analytical and Experimental Analysis of Factors Affecting Exhaust System Performance in Sea Level Static Jet Engine Test Facilities, Ae.E. Thesis, Naval Postgraduate School, Monterey, California, December 1972.
7. National Aeronautics and Space Administration Report CR-419, Non-Isoenergetic Turbulent ($P_{rt} = 1$) Jet Mixing Between Two Compressible Streams at Constant Pressure, by H. H. Korst and W. L. Chow, April 1966.
8. Aerospace Research Laboratories Report No. ARL TR 75-0205,, WPAFB, Performance Characteristics of Ejector Devices, by S. H. Hasinger, June 1975.
9. Naval Postgraduate School Report No. NPS-57Nt-75101, An Investigation of the Flow in Turbojet Test Cells and Augmentors, by J. D. Hayes and D. W. Netzer, October 1975.
10. Croft, D. R. and Lilley, D. G., "Finite-Difference Performance Analysis of Jet Pumps", AIAA Journal, Vol. 14, No. 10, pp 1347-1348, October 1976.
11. Naval Postgraduate School Report No. NPS-67Nt-77091, A Sub-Scale Turbojet Test Cell for Evaluations and Analytical Model Validation, by H. W. Hewlett, P. J. Hickey, and D. W. Netzer, September 1977.
12. Tower, P. W., The Dependence of Compressor Face Distortion on Test Cell Inlet Configuration, Ae.E. Thesis, Naval Postgraduate School, Monterey, California, December 1972.
13. Zucrow, M. J. and Hoffman, J. D., Gas Dynamics, v. 1, p. 194-196, Wiley, 1976.

DISTRIBUTION LIST

	No. of Copies
1. Library Code 0142 Naval Postgraduate School Monterey, CA 93940	2
2. Department of Aeronautics Code 67 Naval Postgraduate School Monterey, CA 93940 R. W. Bell, Chairman D. W. Netzer	1 10
3. Dean of Research Code 012 Naval Postgraduate School Monterey, CA 93940	1
4. Defense Documentation Center Cameron Station Alexandria, VA 22314	2
5. Chief of Naval Operations Navy Department Washington, DC 20360 (Attn: Codes: OP451, OP453)	2
6. Chief of Naval Material Navy Department Washington, DC 20360 (Attn: Codes: 08T241, 044P1)	2
7. Commander Naval Air Systems Command Washington, DC 20361 (Codes: AIR-01B, 330D, 340E, 4147A, 50184, 5341B, 53645, 53651)	8
8. Commanding Officer Naval Air Rework Facility Naval Air Station North Island San Diego, CA 92135 Code: 64279	1
9. Commander Naval Facilities Engineering Command 200 Stovall Street Alexandria, VA 22334 (Codes: 104, 0325)	2

	No. of Copies
10. Naval Construction Battalion Center Pcrt Hueneme, CA 93043 (Codes: 25, 251, 252)	3
11. US Naval Academy Annapolis, MD 21402 (Attn: Prof. J. Williams)	1
12. Arnold Engineering Development Ctr. Arnold AFS, TN 37342 (Code: DYP)	1
13. Air Force Aero Propulsion Laboratory Wright-Patterson AFB, OH 45433 (Code: SFP)	1
14. Detachment 1 (Civil & Environmental Engineering Division Office) HQ ADTC (AFSC) Tyndall AFB, FL 32401 (Code: EV, EVA)	2
15. Army Aviation Systems Command P. O. Box 209 St. Louis, MO 63166 (Code: EQP)	1
16. Eustis Directorate USA AMR & DL Ft. Eustis, VA 23604 (Code: SAVDL-EU-TAP)	1
17. National Aeronautics and Space Admin. Lewis Research Center 2100 Brookpark Road Cleveland, OH 44135 (Attn: Mail Stop 60-6 (R. Rudley))	1
18. Federal Aviation Administration National Aviation Facility Experimental Ctr. Atlantic City, NJ 08405	
19. Naval Air Propulsion Test Center Trenton, NJ 08628 (Code PE71:AFK)	3